PHYSICAL REVIEW A VOLUME 6, NUMBER 1 JULY 1972

Gravity Effects near the Gas-Liquid Critical Point

P. C. Hohenberg and M. Barmatz

Bell Laboratories, Murray Hill, New Jersey 07974

(Received 16 December 1971)

The "linear-model" parametric equation of state of Schofield, Litster, and Ho is used to analyze the effect of gravity near the gas-liquid critical point of a fluid. Detailed results are presented on the density distribution as a function of height, the constant-volume specific heat, and the low-frequency sound velocity, for arbitrary points in the (ρ, T) plane near the critical point. The influence of gravity on the determination of critical exponents is also considered. It is concluded that even for the thinnest practical samples, gravity corrections may have a significant effect on the exponents. The present theory permits gravity corrections to be made in a self-consistent way, with high accuracy.

I. INTRODUCTION

In order to obtain reliable experimental values for critical exponents near phase transitions, it is essential to be able to estimate the various "rounding" effects which smear the transition in any real system. These effects may be due to inhomogeneities, finite-sample effects, impurities, or nonequilibrium behavior. One of the most important rounding mechanisms is the density inhomogeneity caused by gravity at the gas-liquid critical point of a fluid. This effect is substantial since the isothermal compressibility diverges at the critical point, so that a finite density difference will arise from a small pressure difference $\Delta p = \rho g \Delta h$. Thus at the critical temperature $T = T_c$, only one level of a fluid sample will be at the critical point $\rho = \rho_c$. Thermodynamic measurements carried out over a finite sample will average over a region of the (ρ, T) plane, whose extent depends on the precise way in which the compressibility diverges. In contrast to the other rounding mechanisms mentioned above, it is possible to calculate the effect of gravity near the critical point exactly, if the equation of state of the fluid is known. On the other hand, it is often precisely this equation of state which the thermodynamic measurements seek to determine, so that a self-consistent calculation must be performed in order to make reliable gravity corrections.

Although the importance of the gravity effect near T_c was recognized as early as 1892 by Gouy,[1] it was not until 1952 that the first quantitative analysis was presented by Weinberger and Schneider,[2] in connection with their experiments on the coexistence curve and equation of state of xenon. A comprehensive theory of the gravity effect, based on the van der Waals equation of state, was presented by Baehr,[3] who was able to explain the main qualitative effects of gravity. When it became clear, in recent years, that the van der Waals equation was not quantitatively correct near T_c, a number of different analyses of the gravity effect were proposed, using a more realistic equation of state. The work of Berestov, Giterman and Malyshenko,[4-6] was based on a van der Waals-like equation, modified to allow for a divergent specific heat C_v. More recently, a number of proposals based on scaled equations of state have been presented, and analyses of the specific heat in gravity carried out.[7-9] Generally speaking, the explicit equations of state used for these calculations have been either unrealistic, or somewhat cumbersome to manipulate. In particular, many such equations do not incorporate all the known critical exponents, and they lead to spurious singularities in certain thermodynamic functions away from T_c.[10] The equation of state used by Schmidt,[9] on the other hand, has only very weak spurious singularities, and it is known to yield an accurate representation of most thermodynamic functions.[11] However, it cannot be manipulated in closed form for arbitrary points in the (ρ, T) plane, and it is consequently not very well suited for detailed calculations of the gravity effect.

Recently, Schofield, Litster, and Ho[12] presented a simple model equation of state, based on the general parametric representation[12a] of scaling laws introduced by Josephson[13] and Schofield.[14] The parametric representation leads to thermodynamic functions which are free of spurious singularities, and the particular equation proposed in Ref. 12 has an extremely simple form, which leads to tractable expressions for thermodynamic functions in the whole (ρ, T) plane. Moreover, as was shown by Schofield *et al.*,[12] this equation of state fits known experimental data on a large class of magnetic and fluid systems. In the present work we apply this equation to an analysis of gravity effects on various measurable quantities, in particular the coexistence curve, the constant-volume specific heat, and the adiabatic sound velocity.[15] As is discussed in detail in what follows, our primary aim is to obtain accurate estimates of the *corrections* due to the gravity effect, and not to find an exact equation of state. Thus, even if further experi-

mental information forces a refinement of the model equation of Schofield *et al.*,[12] it is probable that the gravity corrections based on this equation will not be substantially modified.

One of the main problems in analyzing experimental data near the critical point, is the determination of the value of T_c, since small shifts in T_c can significantly change the "best-fit" exponents. This point has been emphasized recently by Voronel' and co-workers.[16] One possible choice for T_c is the point at which the specific heat reaches its maximum value, or the sound velocity its minimum. In the present work we study the deviation of this "apparent T_c" from the true critical temperature, as a function of sample height. Another method frequently employed to determine the critical temperature, is to perform a least-squares fit to the data treating T_c as an adjustable parameter. We have investigated the validity of such a procedure by treating the gravity-averaged specific heat as "experimental data" and determining the best-fit values for the exponent α and the temperature T_c. We find that gravity corrections as small as 1 or 2% can significantly shift T_c from its true value, and can lead to systematic shifts in α of the order of ± 0.04.

In Sec. II, the "linear-model" equation of state of Schofield, Litster, and Ho[12] is introduced, and its validity for real fluids briefly discussed. Section III contains a general discussion of the effect of gravity, based on the linear model. The density distribution in a cylindrical vessel of height h is calculated for arbitrary values of the temperature T and average density $\tilde{\rho}$, near T_c and ρ_c, respectively. In Sec. IV, the average specific heat $\tilde{C}_v$ is calculated, and detailed numerical results are presented for xenon. Section V describes calculations of the average sound velocity, based on a numerical solution of the wave equation in an inhomogeneous medium. Results are presented for He^4 over a wide range of temperatures, average densities, and sample heights. In Sec. VI, analyses are presented for various critical exponents, arising from a fit to gravity-averaged quantities, treated as experimental data. Section VII contains a brief summary and conclusion. Most of the detailed computations are discussed in the Appendixes: Appendix A contains the expressions for thermodynamic quantities in terms of the variables r and θ of the "linear model." In addition, the dimensionless units employed throughout this work are described. In Appendix B, the "linear-model" parameters are determined for a number of fluids, Xe, He^4, CO_2, and O_2. Appendix C contains details of the calculation, given in Sec. III, of the density distribution in a vessel, for given values of temperature and average density. In Appendix D, the specific-heat averages are carried out explicitly, and cast into a form which is readily calculated on the computer. In each case certain limits are discussed in which the calculations simplify, such as the case of weak gravity effect, or the critical isotherm ($T = T_c$), or the critical isochore ($\tilde{\rho} = \rho_c$). Appendix E contains a discussion of the numerical solution of the wave equation, leading to the average sound velocity $\tilde{u}$.

II. PARAMETRIC REPRESENTATION

As was pointed out by Josephson[13] and Schofield,[14] the most convenient representation for scaled equations of state is one in terms of parametric variables r and θ, where r is essentially the "radial" distance to the critical point, and θ describes an "angular" position, in the (ρ, T) plane. All critical singularities occur in the variable r, and the dependence on θ is smooth, thus ensuring that known analyticity requirements[10] will not be violated. Specifically we define r and θ by the relations[17]

$$\frac{\mu(\rho, T) - \mu_0(T)}{P_c/\rho_c} \equiv \Delta\mu = a\theta(1-\theta^2)r^{\beta\delta}, \tag{2.1}$$

$$\mu_0(T) = \mu(\rho_c, T), \tag{2.1a}$$

$$(T - T_c)/T_c \equiv t = (1 - b^2\theta^2)r, \tag{2.2}$$

$$b > 1, \tag{2.2a}$$

in terms of the usual exponents β and δ, and the numerical constants a and b, to be determined from experimental data (see Appendix B). The scaled equation of state may then be written in the general form

$$(\rho - \rho_c)/\rho_c \equiv \Delta = \mathcal{K}(\theta)r^{\beta}, \tag{2.3}$$

where $\mathcal{K}(\theta)$ is an unknown polynomial, to be determined. Following Schofield, Ho, and Litster,[12] we shall use the very simple "linear-model" ansatz,

$$\Delta = k\theta r^{\beta}, \tag{2.3a}$$

where k is a positive constant. This ansatz seems to be quite adequate to fit presently available experimental data on fluids and magnetic systems, but there is strong evidence that it is not exact, even for the Ising model in two and three dimensions.[18] The great advantage of the representation (2.1)–(2.3) is that it leads to closed form expressions for all thermodynamic functions. Indeed, using the relation for the chemical potential

$$\mu = \left(\frac{\partial A}{\partial \rho}\right)_T, \tag{2.4}$$

we may integrate Eq. (2.1) to find the free energy $A(\rho, T)$. The remaining thermodynamic functions are then obtained, in terms of r and θ, using the definitions [Eqs. (2.1)–(2.3)] and the standard thermodynamic formulas. Appendix A contains expressions for the functions we shall use, as well as an

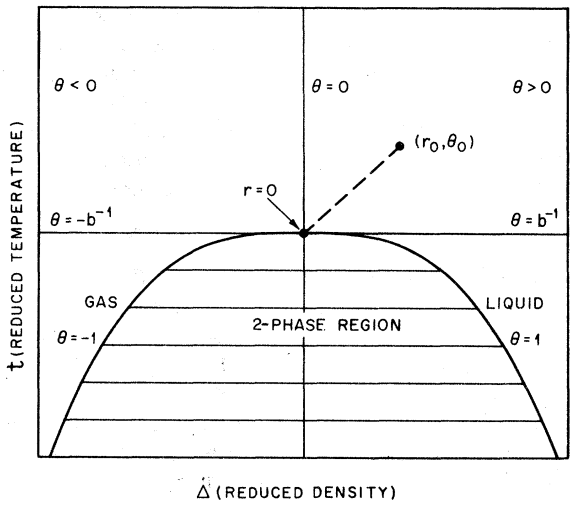

FIG. 1. Schematic representation of the (ρ, T) [or (Δ, t)] plane near the critical point in terms of the parametric variables r, θ. The coordinate r describes the "radial" distance to the critical point, and θ is an angular variable which goes from +1 (liquid branch of coexistance curve) to −1 (gas branch). The critical isotherm has $\theta^2 = b^2$, with $\theta > 0$ for the liquid. The critical point is defined by $r = 0$.

explanation of the dimensionless units we employ throughout this work.

It follows from Eqs. (2.1)–(2.3), that the critical isotherm ($t = 0$) is given by $\theta^2 = b^{-2}$, with $\theta > 0$ for $\rho > \rho_c$, and $\theta < 0$ for $\rho < \rho_c$. The critical isochore above T_c ($t > 0$) is the line $\theta = 0$, and the coexistence curve is the line $\theta^2 = 1$, with $\theta = +1$ being the liquid, and $\theta = -1$ the gas. A schematic representation of the ρ-T plane in terms of the parametric variables is shown in Fig. 1.

The constants a and k are determined by fitting experimental data on the compressibility along the critical isochore (for $T > T_c$), and on the shape of the coexistence curve (see Appendix B). This leaves the constant b, for which we may use the properties of the critical isotherm, or the compressibility along the critical isochore below T_c. As noted in Ref. 12, however, it turns out that there is considerable uncertainty in the experimental data on the latter quantities, so that within the present error limits we may choose b^2 by some other criterion. In Ref. 12, the "minimization" condition

$$b^2 = (\delta - 3)/(\delta - 1)(1 - 2\beta) \tag{2.5}$$

was proposed, since it leads to some simplifications in the thermodynamic functions. We have used this choice for b^2 in most of our numerical calculations, but have worked out the thermodynamic functions for the general case, since experimental data may one day improve sufficiently to favor some different value. In Table I, we present the parameters of the "linear model" for a number of pure fluids.

The main assumptions involved in the use of the present equation of state, besides scaling, the existence of pure power-law divergences and the linear ansatz (2.3a), are the symmetry of the system about $\rho = \rho_c$, and the absence of singular correction terms to the leading asymptotic behavior. These last two assumptions, which are related, are reasonably consistent with presently available experimental data.[11] These assumptions are almost certainly not exactly correct for real fluids, however, and as experiments improve, the necessity for a more sophisticated analysis will become apparent. Theoretical attempts to describe more general nonsymmetric equations of state have been presented by Green, Cooper, and Levelt Sengers,[19] by Widom and Rowlinson,[20] and by Mermin and Rehr,[21] but it is premature to compare these theories with experimental data, in most cases.

It is important to note, of course, that the specific values obtained for the exponents of the leading asymptotic behavior, are extremely sensitive to the choice of correction terms, and the present "best values" may change considerably in the future. One case, which is of particular interest to us, in which present experiments[22] already strongly favor singular correction terms, is the specific heat C_v for CO_2 along ρ_c, where the best fit to

$$C_v = A|t|^{-\alpha} + B_0, \quad t > 0 \tag{2.6a}$$

$$C_v = A'|t|^{-\alpha} + B_0', \quad t < 0 \tag{2.6b}$$

has $B_0 \neq B_0'$. This form implies a singular correction to the leading asymptotic behavior of C_v

$$\delta C_v(t) = (B_0' - B_0)\eta(t), \tag{2.6c}$$

where $\eta(t) = 0$ for $t > 0$, and $\eta(t) = 1$ for $t < 0$. The presence of such a contribution in C_v will lead to corresponding singular correction terms in other thermodynamic functions which can almost certainly not be neglected in any quantitative analysis of critical exponents.[23]

In the present work we are interested in making quantitative estimates of gravity corrections. For this we need expressions for the thermodynamic functions which are *numerically* accurate over the experimental range of density and temperature. Since gravity effects are only important very near T_c, we are only considering explicitly in the analysis the leading singularities, and assuming that the correction terms, whatever their precise form may be, are unaffected by gravity. We believe that the "linear model" provides a sufficiently accurate interpolation between the measured singularities along specified paths, to yield a reliable estimate of the gravity effects. The question of

TABLE I. "Linear-model" parameters for various fluids. Unless otherwise stated all parameters are those of Ref. 11.

Parameter	Xe	CO_2	He^4	O_2
T_c(°K)	289.75	304.12	5.1884	154.576[a]
P_c (dyn/cm^2)	5.83×10^7	7.375×10^7	2.274×10^6[b]	5.043×10^7[c]
ρ_c (g/cm^3)	1.11	0.466	0.0693	0.4362[a]
β	0.351	0.347	0.359	0.353[a]
γ	1.248[d]	1.241[d]	1.212[d]	1.247[a]
α	0.05[e]	0.065[e]	0.07[e]	0.047[d]
δ	4.556[d]	4.576[d]	4.376[d]	4.533[d]
B	1.795	1.983	1.435	1.819[a]
Γ	0.059	0.053	0.13	0.0526[a]
D	3.445[f]	2.666[f]	3.477[f]	3.725[f]
Γ/Γ'	4.29[g]	4.36[g]	4.01[g]	4.24[g]
A_0'	6.02	6.98	3.92[b]	...
μ_0'	−6.47[h]	70.31[i]	−2.6[e]	...
A_0''	78.60[e]		11.95[e]	...
a	23.30	28.37	8.256	26.60
k	1.375	1.492	1.073	1.399
b^2	1.468	1.440	1.445	1.476
U_N (cm/sec)[j]	7.280×10^3	1.258×10^4	5.723×10^3	1.071×10^4
C_N (J/mole °K)[j]	2.40	2.29	2.53	1.19

[a]L. A. Weber, Phys. Rev. A 2, 2379 (1970).
[b]H.A. Kierstead, Phys. Rev. A 3, 329 (1971).
[c]L. A. Weber, J. Res. Natl. Bur. Std. (U.S.) 74A, 93 (1970).
[d]Obtained from scaling.
[e]Fit of linear model to expermiental data at $|t| = 10^{-3}$.
[f]Calculated from Eq. (B7).
[g]Calculated from Eq. (B8).
[h]Reference 29.
[i]Value for $A_0'' + \mu_0''$, obtained by fitting to data of Ref. 22 at $t = 10^{-3}$. The values of A_0'' and μ_0'' are not known separately.
[j]$C_N = (P_c w/T_c\rho_c)\times10^{-7}$; $U_N = (P_c/\rho_c)^{1/2}$.

correction terms to the leading asymptotic behavior is discussed further in Appendix B.

III. EFFECT OF GRAVITY

As was discussed by Edwards, Lipa, and Buckingham[24] the gravitational force can lead to two distinct types of effects on thermodynamic properties near T_c. The first is an explicit dependence of thermodynamic functions on spatial gradients in the system, and the second the spatial variation of thermodynamic functions caused by their dependence on the *local* values of the variables. The explicit effect should only become important when a characteristic length in the system becomes comparable to the correlation length ξ. Let us choose for the characteristic length the quantity

$$\lambda_\rho = \left[\rho^{-1}\left(\frac{d\rho}{dz}\right)\right]^{-1}, \tag{3.1}$$

describing local variations in the density. Then we can verify (see below), that for attainable temperature intervals, say $|t| > 10^{-6}$, we always have

$$\lambda_\rho > 10^2\xi, \tag{3.2}$$

so that spatial gradients can indeed be neglected. Another characteristic length for the system is the smallest dimension h of the container.[22] The requirement $h > 10^2\xi$, say, thus imposes a limitation on the size of the vessel, which for $|t| \geq 10^{-6}$, is roughly $h > 0.05$ cm.

Turning to the implicit effects of gravity, namely, the dependence on local values of thermodynamic variables, we wish to compare the variation of the density, say, between the top and bottom of the vessel, to its average value. Since the compressibility diverges strongly at the gas-liquid critical point, it is clear that close to T_c the effect of gravity must become important, since substantial density gradients can develop. For a given height h, we may *estimate* the temperature interval at which this occurs, by equating the pressure drop $\rho_c gh$ due to gravity, to the quantity

$$\Delta p = [\rho_L(t) - \rho_c]/\rho_c\kappa_T(t), \tag{3.3}$$

where $\rho_L(t)$ is the density of the liquid at temperature t and κ_T is the isothermal compressibility. Inserting the expressions for ρ_L and κ_T from Eqs. (B1) and (B2), of Appendix B into the relation $\Delta p = \rho_c gh$ we may solve for t, which yields

$$t_0(h) = (\Gamma\rho_c gh/BP_c)^{1/\beta\delta}, \tag{3.4}$$

where P_c is the critical pressure, Γ and B are numbers of order unity defined in Eqs. (B1) and (B2), and g is the acceleration of gravity. The values of t_0 we obtain for various fluids are shown in Table II.[25] It is clear from Eq. (3.4) that by employing thin samples one can reduce t_0 and thus

TABLE II. Parameters for the gravity effect. t_0 and $\tilde{\Delta}_0^*$ calculated from Eqs. (3.4) and (3.16), respectively. t_1 is defined as the temperature at which $|\tilde{C}_v - C_v^0|/C_v^0 = 10\%$ for $T > T_c$.

Parameter	Xe	CO_2	He^4	O_2
$h = 0.1$ cm				
t_0	3.1×10^{-5}	1.9×10^{-5}	6.6×10^{-5}	1.8×10^{-5}
$\tilde{\Delta}_0^*$	0.034	0.029	0.033	0.028
t_1	3.4×10^{-5}	1.5×10^{-5}	8.2×10^{-5}	···
$h = 1$ cm				
t_0	1.3×10^{-4}	8.0×10^{-5}	2.9×10^{-4}	7.4×10^{-5}
$\tilde{\Delta}_0^*$	0.057	0.048	0.057	0.047
t_1	1.5×10^{-4}	6.7×10^{-5}	3.65×10^{-4}	···
$h = 10$ cm				
t_0	5.5×10^{-4}	3.4×10^{-4}	1.2×10^{-3}	3.1×10^{-4}
$\tilde{\Delta}_0^*$	0.095	0.080	0.096	0.078
t_1	6.8×10^{-4}	3×10^{-4}	1.7×10^{-3}	···

minimize the implicit gravity effects. However, as mentioned above, in order to avoid explicit effects we must have $h \gg \xi$. Thus, even under ideal conditions it is not possible to eliminate gravity completely, and in practice gravity has almost always been an important factor in past experiments at the critical point. As will be shown below, use of the parametric equation of state permits one to calculate these effects to great accuracy, within the assumption of local thermodynamics, i.e., neglecting the previously mentioned explicit effects.

One method which has been widely used to avoid gravity effects, is to stir the sample at a uniform rate.[5,26] This device, which has the added advantage of reducing the equilibration time significantly, may indeed lead to improvements in experimental convenience, but it is not entirely clear what additional effects the stirring may produce. It would be interesting to make precise measurements with and without stirring, and to analyze the difference, using the present theory.

Under the effect of gravity, the chemical potential depends on the vertical coordinate z, according to the relation

$$d\mu = g\,dz\,. \tag{3.5}$$

Integrating this equation and using Eq. (2.1) we obtain

$$z - z_0 = -(P_c/\rho_c g)a\theta(1-\theta^2)r^{\beta\delta}, \tag{3.6}$$

where z_0 is an integration constant, which we may take to be zero by choosing the origin of z at the point at which $\mu = \mu_0$, i.e., $\rho = \rho_c$. If our system is enclosed in a vessel of height h, we may measure z in units of h, so that Eq. (3.6) becomes

$$z = -x_1\theta(1-\theta^2)r^{\beta\delta}\,, \tag{3.7}$$

$$x_1 = aP_c/\rho_c g h\,. \tag{3.8}$$

Equation (3.7), together with the expression for r [Eq. (2.2)], can be inverted to define a function $\theta(t, z)$. Since all thermodynamic functions are expressible in terms of θ and r, they can therefore be written, at fixed t, as functions of the vertical height z. For example, the density profile is given by

$$\rho(z) - 1 = \Delta(z) = k\theta r^B = k\theta(t,z)\{t/[1 - b^2\theta^2(t,z)]\}^\beta\,. \tag{3.9}$$

(As explained in Appendix A, the density ρ is measured in units of ρ_c.) In Fig. 2, we show the density profile for helium at various temperatures near T_c. Because of the diverging compressibility, the density gradient $(d\rho/dz)_t$ becomes infinite for $T = T_c$ ($t = 0$), but of course this only happens at the single point $z = 0$, at which $\rho = \rho_c$.

Using Eq. (3.9), we may verify that in practice the density gradient does not become large enough for the explicit effects of gravity to manifest themselves. The characteristic dimension λ_ρ for density variations, defined in Eq. (3.1) can be evaluated along the critical isochore, using Eq. (C2) of Appendix C. We find

$$\lambda_\rho = k^{-1}x_1 t^\gamma\,. \tag{3.10}$$

Since this length goes to zero as $t \to 0$ ($T \to T_c$), λ_ρ will eventually become comparable to the correlation length ξ. In practice, however, the reduced temperature never goes below about 10^{-6}, in which case the xenon parameters of Table I would yield

$$\lambda_\rho = 0.03\ \text{cm} \approx 10^2\xi\,,\quad t = 10^{-6}\,,\quad \rho = \rho_c\,. \tag{3.11}$$

For a cylindrical vessel, containing a given mass of material, we may determine the coordinates of the top and bottom of the vessel, from the condition that the integral of the local density be equal to the average density. For example, if a mass M of

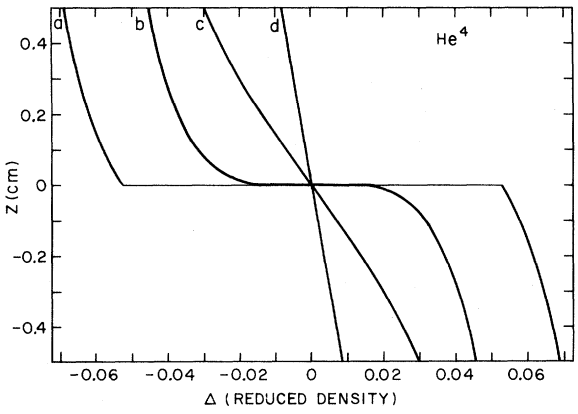

FIG. 2. Density deviation $\Delta = (\rho - \rho_c)/\rho_c$ vs the height z in He^4 for different temperatures near T_c, according to Eq. (2.3a). The reduced temperatures for the different curves are (a) $t = -10^{-4}$, (b) $t = 0$, (c) $t = 3\times10^{-3}$, and (d) $t = 10^{-3}$.

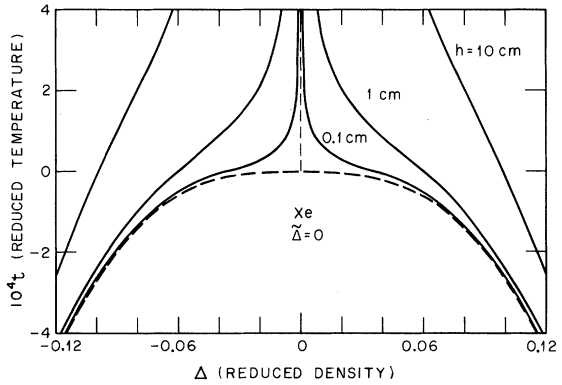

FIG. 3. Density distribution in Xe for different sample heights, when the average density is ρ_c ($\tilde{\Delta}=0$). The solid lines represent the reduced densities [$\Delta \equiv (\rho-\rho_c)/\rho_c$] of the bottom ($\Delta>0$) and the top ($\Delta<0$) of the container. In the limit of zero height, or zero gravity effect, the density vs temperature is given by the dotted line, which coincides with the coexistence curve for $t<0$.

fluid is contained in a vessel of volume V, the average density is

$$\tilde{\rho} = (M/V)\rho_c^{-1} \equiv 1 + \tilde{\Delta} \,. \tag{3.12}$$

Then for each value of t and $\tilde{\Delta}$ the coordinate z_1 of the bottom of the vessel is determined by the condition

$$\tilde{\Delta} = \int_{z_1}^{1+z_1} \Delta(z,\ t)\, dz \,, \tag{3.13}$$

(in our units the height of the vessel is unity). In practice, for each value of t and $\tilde{\Delta}$, we have found the value of z_1 by seeking the zero of the function

$$F(z_1) = \tilde{\Delta} - \int_{z_1}^{1+z_1} \Delta(t,\ z)\, dz \,. \tag{3.14}$$

The numerical procedure we employ is described briefly in Appendix C.

Special Cases

The simplest case is that of a system whose average density is the critical density, i.e., $\tilde{\Delta}=0$. Then since $\Delta(z)$ [Eq. (3.9)] is an odd function of z [as a consequence of the symmetry assumed in Eqs. (2.1)–(2.3)], we see from Eq. (3.13), that

$$z_1 = -\tfrac{1}{2}, \quad \tilde{\rho} = \rho_c \tag{3.15}$$

for all values of t, i.e., the critical density always occurs at the center of the vessel.

Another simple case is $t=0$, when the expression for $\Delta(z)$ simplifies and Eq. (3.13) can be integrated in closed form to find $z_1(\tilde{\Delta})$. This case is discussed in Appendix C.

Given the coordinate z_1, it is a simple matter to evaluate the densities $\Delta_1 = \Delta(z_1)$ and $\Delta_2 = \Delta(1+z_1)$ at the bottom and top of the container. In Fig. 3, we plot these quantities as a function of temperature for Xe, in a system whose average density is $\rho_c(\tilde{\Delta}=0)$, for various sample heights. It is clear from this figure that there is a substantial density variation in the sample near $T=T_c$, even for $h=0.1$ cm. Away from T_c, of course, the density becomes more uniform, except for the finite density jump at the interface which exists in the two-phase region. In Fig. 4, we show the density distribution for average density deviations $\tilde{\Delta}$ equal to 0.02, 0.05, and 0.08. We shall comment later on the characteristic difference between the first two densities and the last one.

Apparent Coexistence Curve

The point $z=0$ has a special significance in our coordinate system. This is the point at which $\rho=\rho_c$, and the maximum density gradient exists in the system. In particular for $t<0$, the gas-liquid interface occurs at $z=0$. For a given $t<0$, there will be a specific value of $\tilde{\Delta}$, at which the interface is at the bottom (or top) of the vessel, i.e., at which $z_1=0$ (or $z_1=-1$). Let us call this value $\tilde{\Delta}^*(t)$, or conversely let $t^*(\tilde{\Delta})$ be the corresponding value of t for given $\tilde{\Delta}$. We may extend the definition of t^* or Δ^* to positive values of t, in which case it is the point of maximum gradient (and not an interface) which is

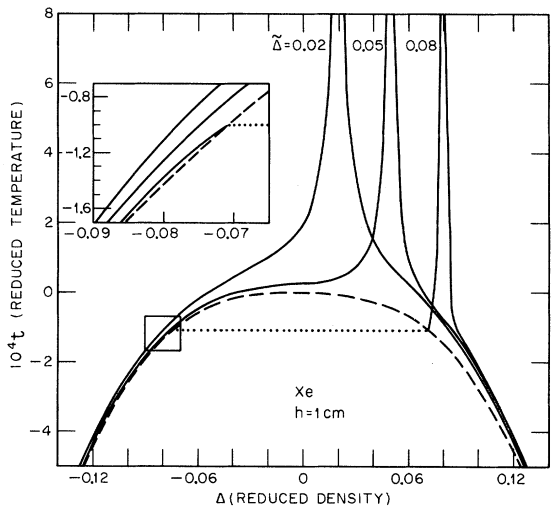

FIG. 4. Density distribution in Xe for $h=1$ cm and different average densities $\tilde{\Delta}$. The dashed line represents the behavior in the absence of gravity, and the solid lines are the reduced densities of the bottom and top of the container in gravity. There is a characteristic difference between the curves for $\tilde{\Delta}<\tilde{\Delta}_0^*=0.057$ and $\tilde{\Delta}>\tilde{\Delta}_0^*$. For $\tilde{\Delta}>\tilde{\Delta}_0^*$, an interface forms inside the container when T is decreased through T_c, and the densities at the bottom and top vary smoothly with temperature. For $\tilde{\Delta}>\tilde{\Delta}_0^*$, the system remains in the one-phase region at $t=0$, and the interface only appears (at the top of the container) at a temperature $t=t^*(\tilde{\Delta})$. The insert shows details of the density distribution on the gas side near $t=t^*(\tilde{\Delta}+0.08)$.

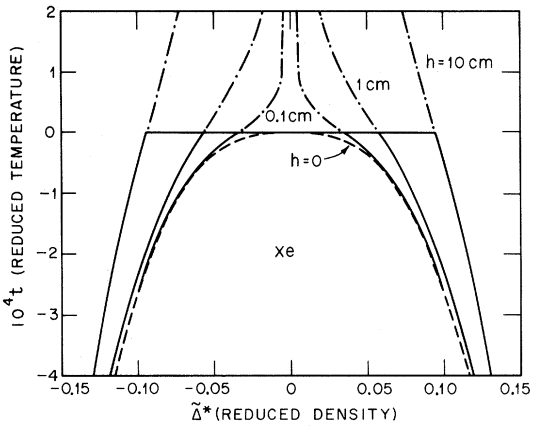

FIG. 5. Average density $\tilde{\Delta}^*(t)$ at which the bottom (or top) of the container is at the critical density, plotted as a function of temperature, for different sample heights, in Xe. For $t \leq 0$, the solid curves play the role of apparent coexistence curves, which approach the true coexistence curve (dotted line) as $h \to 0$. For $t > 0$, the curves are represented by dot-dashed lines. The intercept of the apparent coexistence curve with the critical isotherm $\tilde{\Delta}^*(t=0) = \tilde{\Delta}_0^*$ separates those densities for which the interface forms inside the vessel ($|\tilde{\Delta}| < \tilde{\Delta}_0^*$), from those for which the interface comes in through the bottom (or top) of the vessel ($|\tilde{\Delta}| > \tilde{\Delta}_0^*$), upon cooling through T_c at fixed average density.

at the bottom (or top) of the container when $t = t^*(\tilde{\Delta})$. In Fig. 5, we show the locus of the curves $\tilde{\Delta}^*(t)$ in Xe for various sample heights. It is clear that in the limit of a container of zero height the curve $\tilde{\Delta}^*(t)$ coincides with the coexistence curve, $\pm \Delta_L(t)$ for $t < 0$. For finite sample height, the curve $\tilde{\Delta}^*(t)$ plays the role of an "apparent coexistence curve."

In visual observations, in a system of fixed average density $\tilde{\Delta}$, the meniscus disappears (at $t = 0$) inside the vessel, for $|\tilde{\Delta}| < \tilde{\Delta}^*(t=0)$. For $|\tilde{\Delta}| > |\tilde{\Delta}^*(t=0)|$, on the other hand, the meniscus disappears [at $t = t^*(\tilde{\Delta})$], either through the top of the container (for $\tilde{\Delta} > 0$), or through the bottom (for $\tilde{\Delta} < 0$). This phenomenon has been known for many years, and it was studied quantitatively by Weinberger and Schneider[2] and by Whiteway and Mason.[27] In Fig. 6, we show a comparison of the Xe data[2] with our calculation. For the vertical container ($h = 19.5$ cm) the agreement is satisfactory, within the considerable scatter of the experiment. For the same container in a horizontal position ($h = 1.2$ cm) the data resemble the ideal coexistence curve ($h = 0$), much more than our curve for 1.2 cm (not shown). We provisionally attribute this discrepancy to the stirring which occurred in the experiment, which tends to equalize the densities and remove the gravity effect. In Fig. 7, we have plotted the quantity $\tilde{\Delta}^*(t=0) \equiv \tilde{\Delta}_0^*$ vs height for xenon, along with some experimental points from Refs. 2 and 27. It is interesting to note that the theoretical value of $\tilde{\Delta}_0^*$ goes to zero very slowly, as $h \to 0$, and

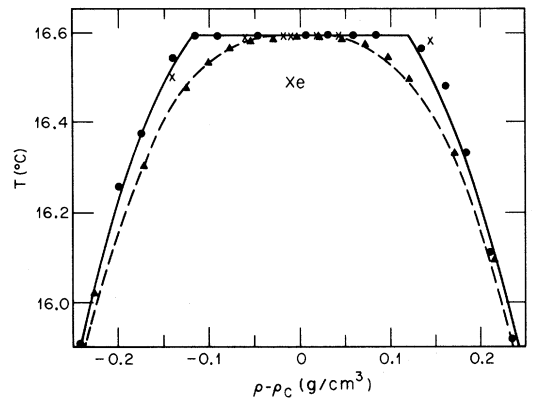

FIG. 6. Apparent coexistence curve vs temperature for $h = 19.5$ cm (solid line) and $h = 0$ (dashed line) in Xe, according to the "linear model." The curves have been plotted in dimensional variables by choosing $T_c = 16.59$ °C and $\rho_c = 1.10$ g/cm^3. The data of Weinberger and Schneider (Ref. 2), are represented by ● and × (for two separate runs) in a vertical container ($h = 19.5$ cm), and by ▲ in the horizontal container ($h = 1.2$ cm). The values of T_c and ρ_c were adjusted for the best fit. The data for $h = 1.2$ cm seem to fit the theory for $h = 0$ better than the theory for $h = 1.2$ cm, which is not shown.

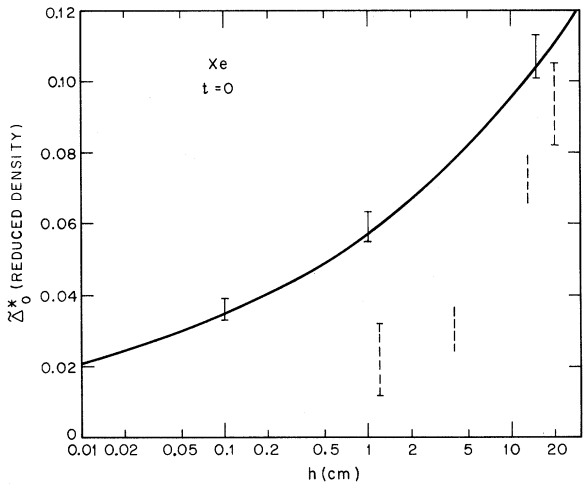

FIG. 7. Reduced density $\tilde{\Delta}_0^*$, which is the $t = 0$ intercept of the solid curves in Fig. 6, plotted as a function of height, in Xe. The solid error bars represent the estimated uncertainty in the parameters D and δ of Eq. (3.16). The dashed lines are experimental data: For $h = 1.2$ and 19.5 cm, the data are those of Weinberger and Schneider (Ref. 2) shown in Fig. 6, with error bars estimated by the authors; for $h = 4$ and 15 cm, the data are those of Whiteway and Mason (Ref. 27), for which no error bars were quoted. Note that the solid curve approaches zero density very slowly as $h \to 0$ (e.g., for $h = 0.1$ cm, $\tilde{\Delta}_0^* \approx 0.035$).

remains equal to 0.03 for $h = 0.1$ cm. From Eqs. (C18), (B3), and (B7) it is easy to show that the quantity $\tilde{\Delta}_0^*$ is completely independent of our model, and only determined by the shape of the critical isotherm, i.e.,

$$\tilde{\Delta}_0^* = \left(\frac{\delta}{\delta+1}\right)\left(\frac{\rho_c g h}{D P_c}\right)^{1/\delta}, \tag{3.16}$$

where D and δ are given in Eq. (B5). Thus the poor agreement shown in Fig. 7 between the experiments of Refs. 2 and 27 on the one hand and Eq. (3.16) on the other, is somewhat disturbing. It seems to us that more precise experimental observations of the apparent coexistence curve for different sample heights would provide an interesting check on the critical parameters of a fluid, and on the equation of state.

Let us comment on the difference mentioned earlier between the curves in Fig. 4. For Xe with $h = 1$ cm, we have $\tilde{\Delta}_0^* = 0.057$, and the curves with $\tilde{\Delta} = 0.02$ and 0.05 correspond to $\tilde{\Delta} < \tilde{\Delta}_0^*$, whereas the curve $\tilde{\Delta} = 0.08$ has $\tilde{\Delta} > \tilde{\Delta}_0^*$. For the first two cases the interface disappears inside the sample when T is raised through T_c, but for $\tilde{\Delta} = 0.08$ the interface leaves the top of the sample (at $t = -10^{-4}$) and the system is in the one-phase region below T_c.

Once the density distribution inside the sample is known for each temperature, the formulas of Appendix A may be used to calculate the spatial dependence of any other thermodynamic function. The procedure which must be employed to find the average of a quantity over the whole sample will depend on the particular experiment performed. As examples of physically interesting quantities which are affected by gravity, we shall discuss the average of the constant-volume specific heat and the low-frequency sound velocity.

IV. GRAVITY AVERAGE OF SPECIFIC HEAT

The constant-volume specific heat as obtained in a standard bulk measurement is not the average of the local C_v over the sample. It is rather equal to the temperature times the derivative with respect to temperature of the average entropy, with the *total* volume of the system held constant. Let $S(t, z)$ be the local value of the entropy. Then the average entropy of a cylindrical container of height h is

$$\tilde{S}(t) = \int_{z_1}^{1+z_1} S(t, z)\, dz, \tag{4.1}$$

where the coordinate z_1 of the bottom of the container has been determined from Eq. (3.13).

The gravity-averaged specific heat is then

$$\rho\tilde{C}_v = T\frac{\partial\tilde{S}}{\partial T} = (1+t)\frac{d}{dt}\tilde{S}(t) \tag{4.2}$$

($\tilde{C}_v$ is a specific heat per unit mass, and $\rho\tilde{C}_v$ is per unit volume, see Appendix A). As mentioned earlier, we shall neglect the spatial variation of the background terms, and only consider the average of the singular parts. Writing

$$\tilde{C}_v = \tilde{C}_v^{\text{sing}} + \tilde{C}_v^{B}, \tag{4.3}$$

we show in Appendix D [Eq. (D4)] that

$$\rho(1+t)^{-1}\tilde{C}_v^{\text{sing}} \equiv \tilde{S}' = \int_{z_1}^{1+z_1}\left(\frac{\partial S_s}{\partial t}\right)_z dz - \left(\frac{S_s(t,\,1+z_1) - S_s(t,\,z_1)}{\Delta(t,\,1+z_1) - \Delta(t,\,z_1)}\right)\int_{z_1}^{1+z_1}\left(\frac{\partial\Delta}{\partial t}\right)_z dz, \tag{4.4}$$

where S_s is the singular part of S [Eq. (A6)]. Using the relation between z and θ [Eq. (3.7)], this expression for $\tilde{S}'$ may be written in terms of integrals over θ, which are given explicitly in Eqs. (D5)–(D7) of Appendix D.

In the limiting case of no gravity (i.e., $h = 0$) it can be shown that the first term on the right-hand side of Eq. (4.4) reduces to $\rho(1+t)^{-1}C_\mu$, whereas the second term reduces to $\rho(1+t)^{-1}(C_v - C_\mu)$. For $t > 0$, and $\rho = \rho_c$ we have $C_v = C_\mu$ so only the first term contributes. For $t < 0$ and $\rho = \rho_c$, the measured C_v in the two-phase region is just the average of C_μ for the gas and the liquid.[28] According to our symmetry assumptions, the quantity ρC_μ has the same value for the gas and the liquid, and once again only the first term in Eq. (4.4) contributes.

More generally, even in the presence of gravity, the second term of Eq. (4.4) does not contribute if the average density is equal to ρ_c (i.e., $\tilde{\Delta} = 0$). These statements are demonstrated in Appendix D, where the full expressions for $\tilde{C}_v$, including the background terms, are derived. We also treat explicitly the special cases $\tilde{\Delta} = 0$ and $t = 0$.

Results for Specific Heat of Xenon

In order to demonstrate the effect of gravity on C_v, we have made an extensive series of calculations for xenon, mostly for a height of 1 cm, which corresponds to the experiment of Edwards *et al.*[24] We have studied both isochores and isotherms, by which we mean, respectively, paths of constant *average* density as a function of temperature, and paths of constant temperature as a function of average density. Since the linear-model parameters do not vary greatly from fluid to fluid, the results for xenon should be semiquantitatively correct for other systems, when expressed in dimensionless form (see Appendix A).

In Fig. 8, we show the specific heat $\tilde{C}_v$ along the critical isotherm ($t = 0$), for various sample heights. In contrast to the gravity-free specific heat, which diverges as $\Delta^{-\alpha/\beta}$ when $\Delta \to 0$, the value in gravity is essentially constant for small $\tilde{\Delta}$. A sharp drop occurs at a characteristic value of $\tilde{\Delta}$, which increases

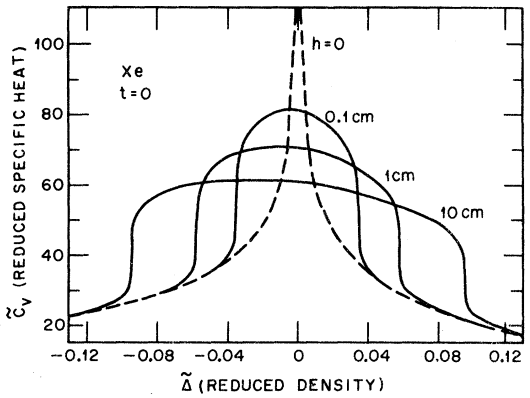

FIG. 8. Average specific heat $\tilde{C}_v$ vs reduced density $\tilde{\Delta}=(\bar{\rho}-\rho_c)/\rho_c$, in Xe along the critical isotherm, for various sample heights. Note the sharp drop in $\tilde{C}_v$ at the value $|\tilde{\Delta}|=\tilde{\Delta}_0^*$ (see Fig. 7), at which the top (or bottom) of the container is at the critical density. The specific heat is expressed in dimensionless units, as explained in Appendix A. In order to obtain $\tilde{C}_v$ in J/mole °K multiply the dimensionless $\tilde{C}_v$ by $C_N=2.4$.

with increasing height. This value is just the quantity $\tilde{\Delta}_0^*$ discussed earlier, at which the point of maximum density gradient ($z=0$, $\rho=\rho_c$) leaves the sample volume. For $t=0$ it can be shown analytically from Eqs. (D17)–(D27) of Appendix D that at $|\tilde{\Delta}|=\tilde{\Delta}_0^*$ the average specific heat has an infinite derivative as a function of $\tilde{\Delta}$. For $|\tilde{\Delta}|>\tilde{\Delta}_0^*$, the density gradients in the sample become smaller, and $\tilde{C}_v$ approaches its gravity-free value.

From the symmetry properties of the assumed equation of state (2.1)–(2.3), it follows that $\rho\tilde{C}_v^{\text{sing}}$ will be symmetric for $\pm\tilde{\Delta}$. Since in practice such symmetry is not observed for the full C_v, we have included an asymmetric term in the background contribution in Eq. (4.3). We have chosen this term to fit the calculated C_v values of Habgood and Schneider,[29] along isochores far from T_c. A more accurate determination of this quantity must await detailed measurements of C_v as a function of density. The asymmetry of $\tilde{C}_v$ which follows from our choice of parameters is apparent in Fig. 8, but since it is completely decoupled from our gravity analysis, we have only shown results for positive $\tilde{\Delta}$ in subsequent figures.

For isotherms with $t>0$, the specific heat varies more smoothly, and has an inflection point at $\tilde{\Delta}=\tilde{\Delta}^*(t)$, with finite first derivative. Since t is positive, the density gradient is everywhere finite in the sample (even at $z=0$), and $\tilde{C}_v$ is smooth. The isotherm $t=+10^{-5}$ is shown in Fig. 9; for larger t values the change in $\tilde{C}_v$ at $\tilde{\Delta}^*(t)$ is less pronounced, since the density gradients are smaller. For isotherms with $t<0$, the specific heat has a finite jump at $\tilde{\Delta}=\tilde{\Delta}^*(t)$, which occurs when the gas-liquid interface leaves the sample. This jump is analogous to the one occurring at the coexistence curve in the absence of gravity which is associated with the latent heat of vaporization. However, in the present case the jump is reduced in magnitude by the gravity effect, and displaced to the "apparent" coexistence curve $\tilde{\Delta}^*(t)$, which lies outside $\Delta_{\text{coex}}(t)$ (see Fig. 5). The isotherm at $t=-10^{-5}$ is also shown in Fig. 9; for lower t, the behavior is closer to that in the absence of gravity.

Although the variation of $\tilde{C}_v$ along isotherms is quite striking, in practice it is generally isochores which are measured, and some of those are shown on a linear temperature scale in Fig. 10. It is apparent from this figure that in the presence of gravity there is a difference between small values of $\tilde{\Delta}$, for which $\tilde{C}_v$ is a smooth function of temperature, and larger values of $\tilde{\Delta}$ for which $\tilde{C}_v$ experiences a jump as a function of t. The dividing value is $\tilde{\Delta}=\tilde{\Delta}_0^*$. The jump in $\tilde{C}_v$ occurs at the temperature $t=t^*(\tilde{\Delta})$, which once again plays the role of an apparent coexistence temperature, for given $\tilde{\Delta}$.

In Fig. 11, we illustrate how sensitive $\tilde{C}_v$ is to the value of $\tilde{\Delta}$, by showing two isochores on either

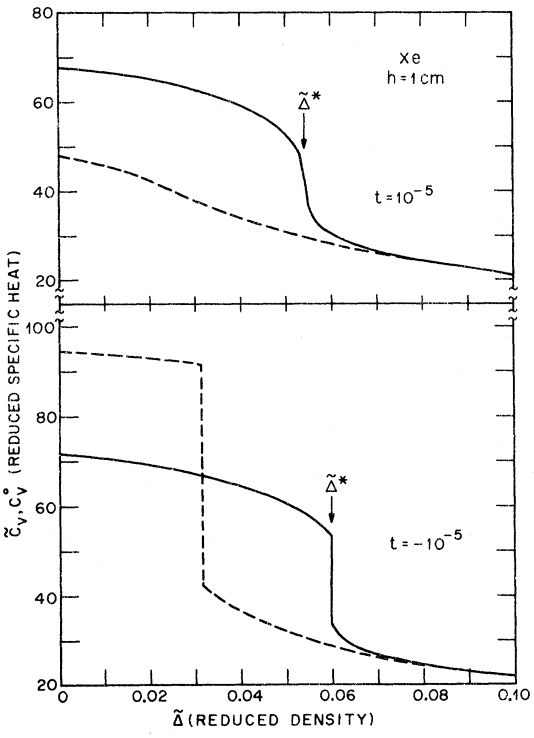

FIG. 9. Average specific heat $\tilde{C}_v$ in dimensionless units (solid curves) vs reduced density $\tilde{\Delta}$ for isotherms $t=\pm 10^{-5}$, compared with the gravity-free value C_v^0 (dashed curves). Only positive density deviations are shown. In the upper figure ($t>0$) the drop in $\tilde{C}_v$ which occurs at $\tilde{\Delta}=\tilde{\Delta}^*(t=10^{-5})$ is less pronounced than for $t=0$. In the lower figure, there is a finite jump in $\tilde{C}_v$ which occurs at the apparent coexistence density $\tilde{\Delta}=\tilde{\Delta}^*(t=-10^{-5})$ (see Fig. 5).

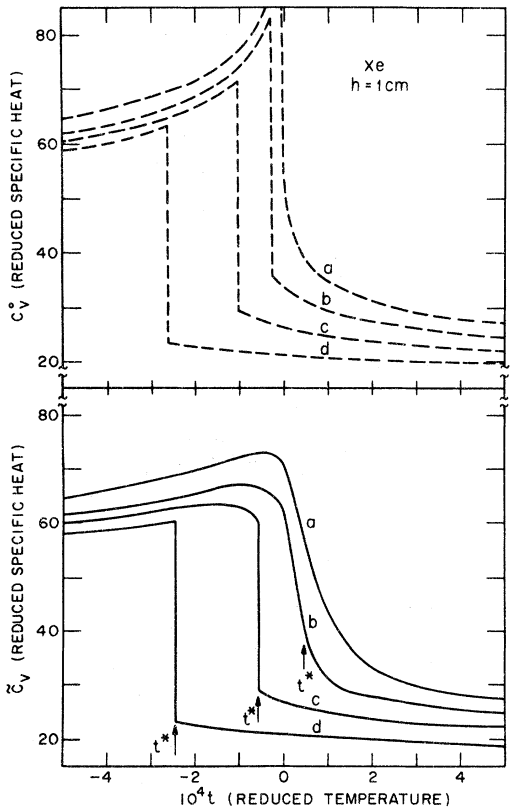

FIG. 10. Specific heat, in dimensionless units, along isochores, plotted on a linear temperature scale. The upper figure shows C_v for zero gravity (or zero height) and the lower figure, the corresponding curves in the presence of gravity. The average densities are (a) $\tilde{\Delta}=0$, (b) $\tilde{\Delta}=0.044$, (c) $\tilde{\Delta}=0.07$, and (d) $\tilde{\Delta}=0.10$. Note the difference in behavior between curves (b) and (c) of the lower figure which correspond to $\tilde{\Delta}<\tilde{\Delta}_0^*$ and $\tilde{\Delta}>\tilde{\Delta}_0^*$, respectively. The temperature at which $\rho=\rho_c$ at the top of the cell is denoted by t^*.

side of $\tilde{\Delta}_0^*=0.057$, namely, $\tilde{\Delta}=0.0565$ and $\tilde{\Delta}=0.058$, for which $\tilde{C}_v$ behaves quite differently. A more complete set of isochores is shown on a logarithmic temperature scale in Figs. 12(a)–12(e), as well as the comparison with the gravity-free specific heat C_v^0. The maximum in $\tilde{C}_v$ along isochores always occurs at temperatures below T_c. The locus of these maxima, shown in Fig. 13, is inside the coexistence curve for small $\tilde{\Delta}$, but it crosses at some value of $\tilde{\Delta}$, and then joins the "apparent" coexistence curve $\tilde{\Delta}(t)$. In the absence of gravity, of course, the locus of specific-heat maxima along isochores is the coexistence curve itself. The locus of specific-heat maxima, and of specific-heat jumps was studied in Ref. 6, based on a van der Waals–like equation of state with logarithmic specific heat, and the results are qualitatively similar to ours. In order to demonstrate how the present results depend on the sample height h, we show in Fig. 14 the variation of the temperature $t_{\max}$ at which $\tilde{C}_v$ attains its maximum along the critical isochore. Also shown, are the values of $\tilde{C}_v$ at $t_{\max}$ and at $t=0$, as a function of sample height.

It is hoped that some of the predictions of the present calculations can be verified by detailed specific-heat measurements. In particular, the significant changes in shape caused by gravity, as shown in Figs. 12(c) and 12(d), should be easily detectable. Also, the locus of the specific-heat maxima and the deviation of this locus from the coexistence curve shown in Fig. 13, would be interesting to investigate experimentally.

The present calculations should also serve to make quantitative gravity corrections, in those cases where the ideal gravity-free behavior is sought. In order for our estimates to be reliable, they should not depend too much on the particular parametrization we used, since in practice there is considerable uncertainty at the present time in the values of B, Γ, D, β, and δ (see Table III and Fig. 15). We have first tested the dependence of $\tilde{C}_v$ on the choice of b^2, by changing its value from Eq. (2.5), normalizing the specific heat to agree with experiment[24] at $t=10^{-3}$. The result for $t=0$ and $\tilde{\Delta}=0$ is shown in Fig. 15(a), where the experimental value from Ref. 24 is also shown. It is interesting to note that the maximum in $\tilde{C}_v$ occurs for the value b_{LM}^2 given by Eq. (2.5), and this choice is consistent with the experiment. However, since $\tilde{C}_v$ only varies by a few percent when b^2 varies within the uncertainties discussed in Appendix B, we see that other choices for b^2 are also permissible.

In addition to a variation with b^2 for given β, δ, B, and Γ, the value of $\tilde{C}_v$ also changes when these latter parameters are varied. In Table III, we show how $\tilde{C}_v$ at $t=0$, $\tilde{\Delta}=0$ varies for the five alter-

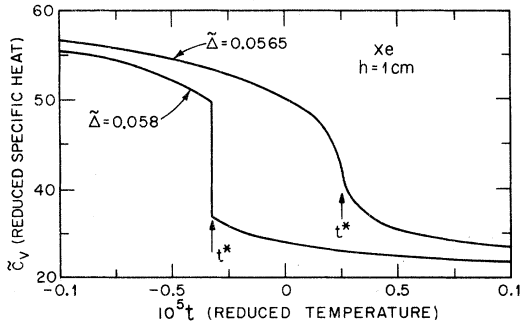

FIG. 11. Average specific heat vs temperature for two isochores near $\tilde{\Delta}_0^*=0.057$. In the upper curve ($\tilde{\Delta}<\tilde{\Delta}_0^*$) the interface forms inside the vessel and the average specific heat varies smoothly as a function of temperature. The lower curve ($\tilde{\Delta}<\tilde{\Delta}_0^*$), whose reduced density only differs from the upper by 0.15%, has a sharp drop at $t=t^*(\tilde{\Delta})$, where the interface enters the top of the sample.

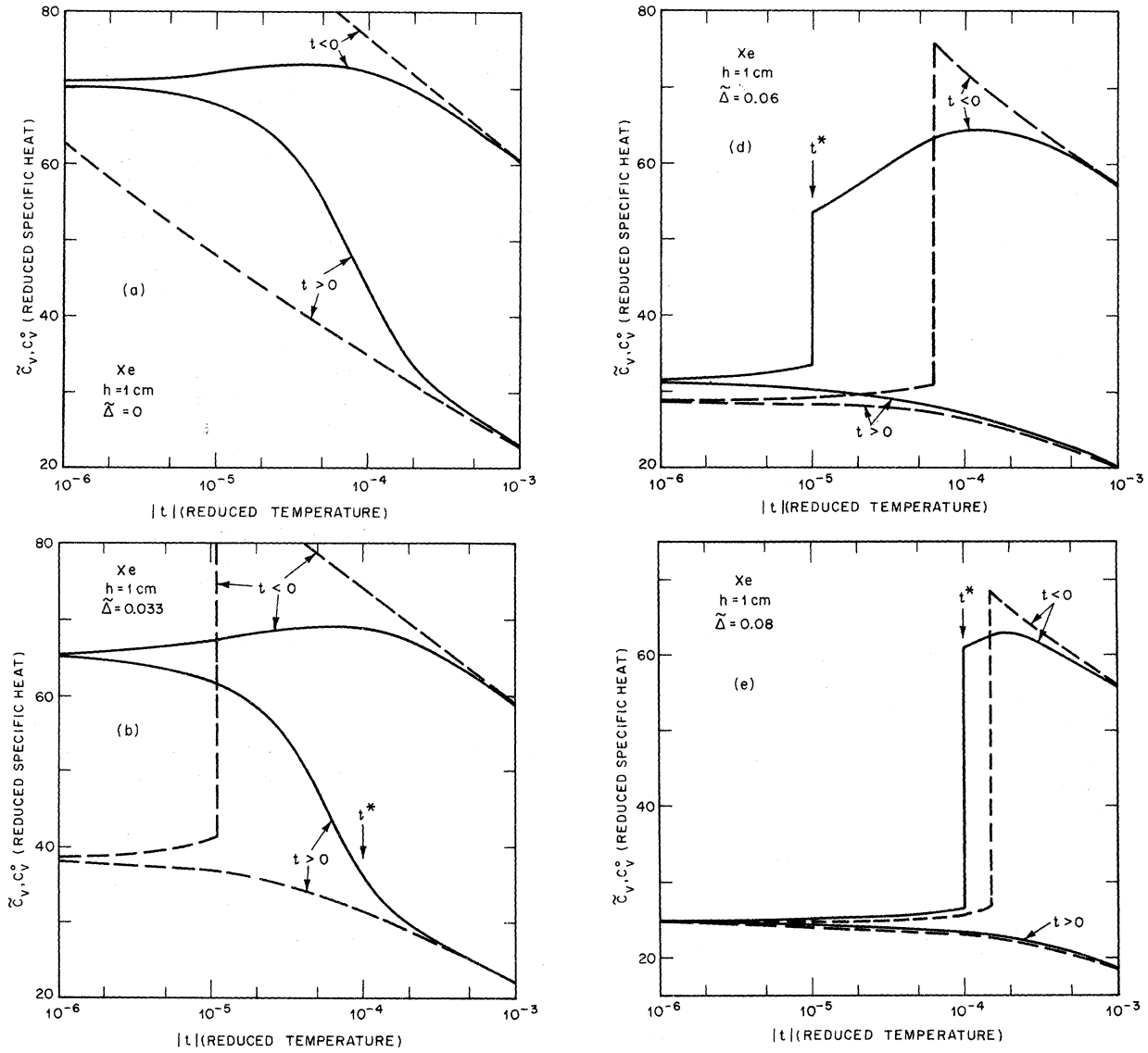

FIG. 12. (a)–(e) The specific heat $\tilde{C}_v$ in gravity (solid curves) and out of gravity (dashed curves) for a number of isochores, plotted as a function of temperature on a logarithmic scale. The temperature at which $\rho = \rho_c$ at the top of the container is denoted by t^*. The specific heats are expressed in dimensionless units.

nate self-consistent sets suggested by Schmidt[9] (the background contribution to $\tilde{C}_v$ was adjusted each time to agree with experiment at $t = 7.94 \times 10^{-4}$). In agreement with Schmidt's conclusion, we see that the value of $\tilde{C}_v$ at this point is not very sensitive to the choice of parameters (see also Appendix B). Thus, experiments on C_v do not at this time provide an unambiguous test of various parametrizations of the equation of state, even within the "linear model." It is hoped, however, that eventually the uncertainties in experimental data and in the param-

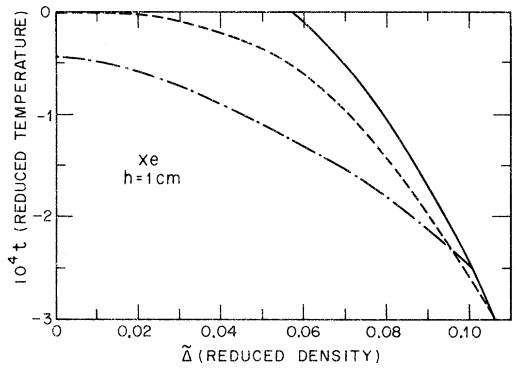

FIG. 13. Locus of specific-heat maxima along isochores in the $(t, \tilde{\Delta})$ plane is shown by the dot-dashed line. The dashed line is the coexistence curve, which is the locus of specific-heat maxima in the absence of gravity. The solid line is the apparent coexistence curve, which is the locus of specific-heat jumps along isochores, in the presence of gravity.

eters of our model can be reduced substantially. In that event, one of the interesting quantities to fit to experiment is the value of $\tilde{C}_v$ at $t=0$, $\tilde{\Delta}=0$ for various heights. Finally, we also show in Table III the variation in the value of $(\tilde{C}_v - C_v^0)/C_v^0$ with the choice of linear-model parameters at $\tilde{\Delta}=0$, $t=1.5\times10^{-4}$, where the gravity effect is significant but not dominant. As can be seen, the results are very insensitive to the choice of parameters, which gives us additional confidence that gravity corrections can be made reliably at least when they are not too large. Similarly, if b^2 is modified from its value b_{LM}^2 given by Eq. (2.5), the percentage deviation $(\tilde{C}_v - C_v^0)/C_v^0$ remains essentially unchanged at $t=1.5\times10^{-4}$.

In order to compare the gravity effect on C_v in various fluids quantitatively, we show in Table II the value of $t_1(h)$, which we define as the reduced temperature for which $|\tilde{C}_v - C_v^0|/C_v^0$ is 10% (we assume $t>0$), for the given height h. From this table, we see that for a given height, the fluids O_2 and CO_2 have the smallest gravity effect.

V. SOUND VELOCITY

The thermodynamic formula for the adiabatic sound velocity is

$$u^2 = (\rho\kappa_S)^{-1} = (\rho\kappa_T)^{-1} + T\rho^{-2}\left(\frac{\partial P}{\partial T}\right)_\rho^2 C_v^{-1} . \qquad (5.1)$$

Since near the critical point κ_T^{-1} goes to zero rapidly and $(\partial P/\partial T)_\rho^2$ goes to a constant, u^2 is proportional to C_v^{-1}, and vanishes with the exponent α along the critical isochore. In practice, two types of corrections have to be applied to Eq. (5.1) near T_c, namely, dispersion and gravity. The first, which is an example of an "intrinsic effect" discussed in Sec. II, arises because there exist slow relaxation processes in the medium, with a relaxation time τ' which diverges at T_c. This leads to corrections to Eq. (5.1) of order $\omega\tau'$ at finite frequencies. Although there does not exist at present an exact theory of dispersion in fluids near T_c, the effects may be estimated experimentally with reasonable accuracy.[30,31] In any case, we shall not discuss these effects further in this paper, but rather turn to the second correction to Eq. (5.1). In the presence of gravity, the sound velocity depends on the position z in the container. The function $u(z)$ is obtained by expressing the thermodynamic functions in Eq. (5.1) in terms of the variables t and $\theta(z, t)$. The "average velocity" for a cylindrical cavity of height h and radius a' is obtained by calculating the eigenfrequencies of the wave equation in the medium,

$$\nabla^2\Phi(\vec{r}', \tau) - \frac{1}{u^2(z)}\frac{\partial^2}{\partial\tau^2}\Phi(\vec{r}', \tau) = 0 , \qquad (5.2)$$

with the boundary condition

$$\vec{\nabla}\Phi = 0 \qquad (5.3)$$

on the boundaries of the cylinder (τ is the time variable; $\vec{r}'$ is the three-dimensional spatial coordinate with cylindrical components r', φ, z; and Φ is the wave function for the sound wave).

As is discussed in Appendix E, the eigenfrequencies of Eq. (5.2) for the inhomogeneous fluid may be classified according to the "quantum numbers" p, m, and n of the cylindrical cavity in a uniform medium. Modes with $p=0$ are calles "Bessel-function" modes, and those with $m=n=0$ are called "plane-wave" modes. The others are "mixed"

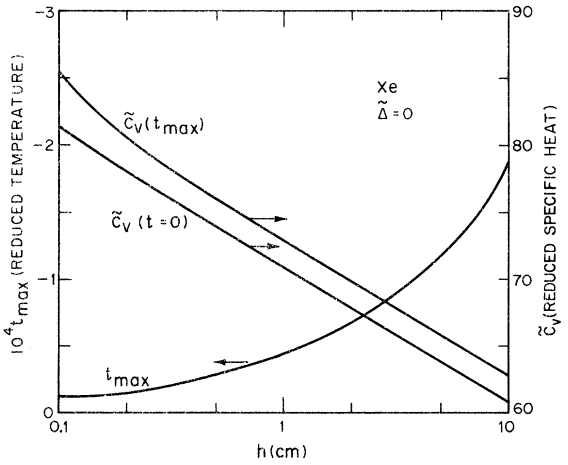

FIG. 14. Position of the specific-heat maximum t_{max} along the critical isochore ($\tilde{\Delta}=0$) in Xe, plotted as a function of sample height on a logarithmic scale. Also shown are the values of the specific heat at $t=0$ and at $t=t_{max}$, for the different heights.

TABLE III. Alternate parameters for Xe. The values of α, β, B, and Γ for columns 2–6 are those of Ref. 9.

α	0.05	0.013	0.04	0.057	0.075	0.09
β	0.351	0.361	0.350	0.350	0.350	0.335
B	1.795	1.897	1.802	1.802	1.802	1.591
Γ	0.059	0.056	0.059	0.063	0.070	0.063
a	23.30	32.59	23.77	21.79	19.22	18.37
k	1.375	1.523	1.395	1.368	1.340	1.163
b_{LM}^2	1.468	1.545	1.481	1.455	1.429	1.392
$A_0'' + \mu_0''$ [a]	72.13	433.81	97.57	56.57	32.32	23.75
$\tilde{C}_v(-t) - \tilde{C}_v(t)$ [b]	37.31	34.41	35.45	37.17	37.54	35.49
$[\tilde{C}_v(-t) - \tilde{C}_v(t)]_{\text{expt}}$ [b,c]	37 ± 0.5	37 ± 0.5	37 ± 0.5	37 ± 0.5	37 ± 0.5	37 ± 0.5
$\tilde{C}_v(t=0,\ \tilde{\Delta}=0)$	70.61	64.03	67.91	70.98	72.32	73.06
$[\tilde{C}_v(t=0,\ \tilde{\Delta}=0)]_{\text{expt}}$ [c]	72 ± 3.5	72 ± 3.5	72 ± 3.5	72 ± 3.5	72 ± 3.5	72 ± 3.5
$(\tilde{C}_v - C_v^0)/C_v^0$ for $t = 1.5 \times 10^{-4}$	0.1246	0.1260	...	...	...	0.1265

[a] Obtained by a fit to data of Ref. 24 at $t = 10^{-3}$.

[b] For $|t| = 7.94 \times 10^{-4}$.

[c] Reference 24.

modes. Most of the velocity calculations presented in this paper are for the lowest order radial mode, $p = m = 0$, $n = 1$. The average velocity for the mode p, m, n is defined in terms of the eigenfrequency ω_{pmn} for that mode, by the relation

$$\tilde{u}_{pmn}^2 \equiv \omega_{pmn}^2 [(\pi \alpha_{mn}/a')^2 + (\pi p/h)^2]^{-1}, \qquad (5.4)$$

where the $\{\alpha_{mn}\}$ are numbers of order unity defined in Appendix E. It is easy to see from the equations of Appendix E that for a uniform medium with sound velocity u_0 the right-hand side of Eq. (5.4) reduces to u_0^2, for all values of p, m, and n.

The method we have used to find the eigenfrequencies of Eq. (5.2) near T_c is described briefly in Appendix E. In the limiting case of a nearly uniform local velocity we may also find the eigenfrequencies by perturbation theory, which is also discussed in Appendix E. We have verified that in this limit the results of the two methods agree.

Let us now turn to a discussion of the results for $\tilde{u}$ as a function of t and $\tilde{\Delta}$. We have chosen He^4 as our system, since this is the fluid under experimental investigation by one of us.[30,31] In Fig. 16, we show $\tilde{u}$ (in dimensionless units) for the 001 mode along an isotherm $t = +10^{-6}$ which is very near critical, for three different sample heights $h = 5$ cm, $h = 0.5$ cm, and $h = 0.1$ cm. These curves are to be compared to the ones in Fig. 8 for $\tilde{C}_v$. The asymmetry between $\tilde{\Delta} > 0$ and $\tilde{\Delta} < 0$ arises from the small asymmetry of the local velocity about $z = 0$. For each curve there is a sharp break near the corresponding value of $\tilde{\Delta}^*$ for $t = 10^{-6}$. Figure 17 shows two other isotherms, at $t = \pm 10^{-4}$. The gravity-free velocity for $t < 0$ has a sharp break when $\tilde{\Delta}$ reaches the coexistence density $\Delta_L(t = -10^{-4})$, and the average velocity [see Eq. (E17)] is essentially independent of $\tilde{\Delta}$ in the two-phase region since $u_L \approx u_G$. In the presence of gravity the behavior is very similar, but shifted to the "apparent coexistence density" $\tilde{\Delta}^*(t = -10^{-4})$.

Turning now to isochores, we show a series of these in Figs. 18, 20(a), and 20(b). The velocity along the critical isochore ($\tilde{\Delta} = 0$) is shown in Fig. 18 for three different modes (100, 001, and 200), along with the gravity-free value, which is of course independent of the mode. From this figure we see that gravity introduces an apparent dispersion, which must be taken into account in any analysis of the true dispersion effects coming from the dynamics of the transition.[31] The apparent dispersion is illustrated further in Fig. 19, where we plot the deviation $(\tilde{u}_p/u_0) - 1$ vs the plane-wave index p, at $\tilde{\Delta} = 0$, $t = 10^{-5}$, for modes with $m = n = 0$. The largest effect (21%) occurs for $p = 1$, and the smallest (17%) for $p = 2$. The Bessel-function modes 001 and 010, indicated by an arrow, have a deviation of $\approx 18\%$ at this point. Figure 20 shows the 001 mode for positive isochores and is to be contrasted with Fig. 10 for the specific heat. The gravity-free velocity experiences a minimum with a cusp at the coexistence curve; this cusp is rounded and displaced by gravity. It is interesting to note that the sign of $\tilde{u} - u_0$ changes between $\tilde{\Delta} = 0.02$ and $\tilde{\Delta} = 0.04$. For the higher isochores, shown in Fig. 20(b), the only effect of gravity is to shift the coexistence curve, as discussed in Sec. III. Generally speaking, the velocity can be measured with great accuracy, and many of the effects described here should be easily observable.

VI. ANALYSIS OF CRITICAL EXPONENTS

In this section we investigate the effect of gravity corrections on the determination of critical exponents. Our point of view is to treat the theoretical gravity-averaged quantities as experimental data,

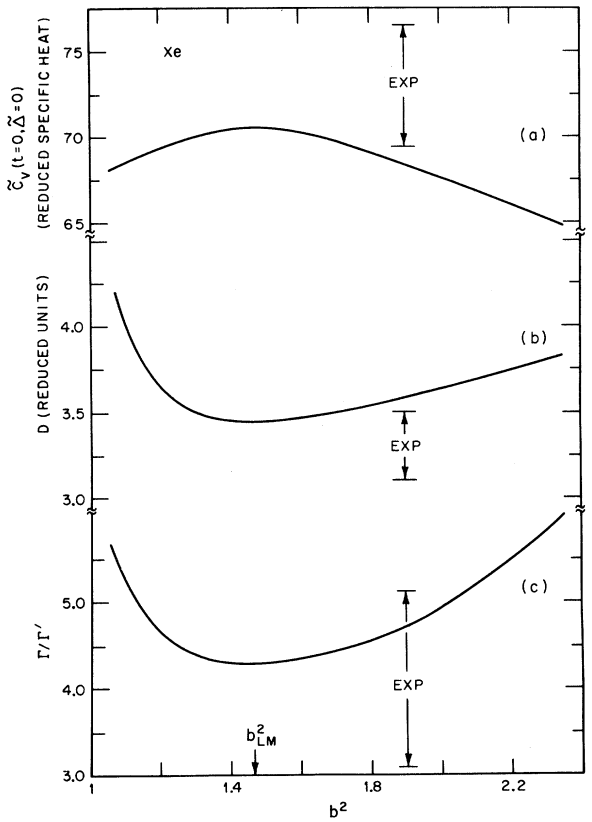

FIG. 15. Test of the sensitivity of our results for Xe to the value of b^2. Curve (a) shows the specific heat $\tilde{C}_v$ at $t=0$, $\tilde{\Delta}=0$ as a function of b^2 (with the other parameters having the values given in Table I), along with the experimental value from Ref. 24 in dimensionless units. The range of b^2 permitted by Eq. (B9) is $1<b^2<3.35$. The constant term A_0' [Eq. (A9)] was adjusted at each value of b^2, to make C_v agree with experiment at $t=10^{-3}$. Note that the value of $\tilde{C}_v$ will also change if β, B, and Γ are changed from the values given in Table I. The maximum in $\tilde{C}_v$ occurs at the value b^2_{LM}, which is the one determined by Eq. (2.5). Curve (b) shows the variation of D [Eq. (B7)], and the experimental value which follows from the analysis of Ref. 11. Curve (c) is the corresponding result for Γ/Γ'. In each case the extremum occurs at b^2_{LM}.

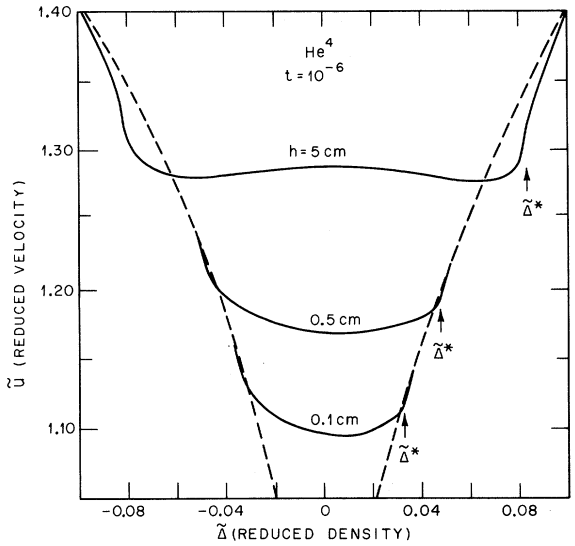

FIG. 16. Average velocity $\tilde{u}$ of the lowest-order radial mode 001 in He^4 for an isotherm which is close to critical, $t=10^{-6}$, and various sample heights, plotted as a function of average density $\tilde{\Delta}$. The dashed line represents the velocity out of gravity. The break in $\tilde{u}$ occurs very near the density $\tilde{\Delta}=\tilde{\Delta}^*(t=10^{-6})$. The velocity is expressed in dimensionless units as explained in Appendix A. In order to obtain $\tilde{u}$ in cm/sec multiply the dimensionless $\tilde{u}$ by $U_N=5.723\times10^3$.

and to perform least-squares fits to determine the best critical exponents and the best value of T_c. We can then compare the results with the starting "ideal" exponents for the corresponding quantities in the absence of gravity. Since there is clearly some arbitrariness in deciding how to treat our "experimental data," the results of the present section are intended primarily for illustrative purposes.

A. Apparent Value of α and α' for Xenon along Critical Isochore

As a first test of the influence of gravity on the exponents, we consider the average specific heat $\tilde{C}_v$ for xenon in a 1-cm container[24] along $\rho=\rho_c$, in the temperature interval $7\times10^{-5}\leq|t|\leq7\times10^{-3}$, where t is referred to the ideal starting T_c, called T_c^0. The maximum value of $|t|$, $t_{max}=7\times10^{-3}$ was chosen as a reasonable though somewhat arbitrary estimate of the point at which correction terms begin to be important.[24] The minimum value was varied for each fit from $|t_{min}|=1.8\times10^{-3}$, down to $|t_{min}|=7\times10^{-5}$, which was chosen as a temperature at which gravity rounding is "clearly" apparent.[24]

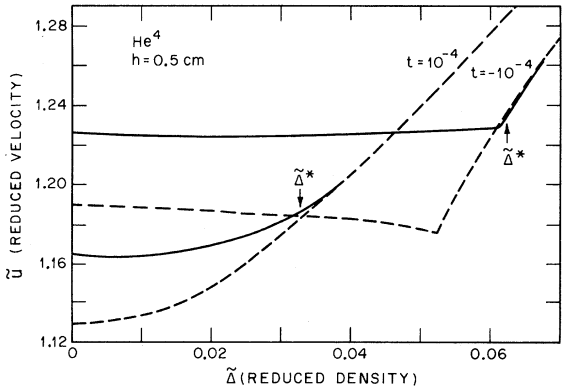

FIG. 17. Average dimensionless velocity of the lowest-order radial mode 001 in He^4 for the two isotherms $t=\pm10^{-4}$, as a function of average density $\tilde{\Delta}$. The dashed lines represent the gravity-free velocity.

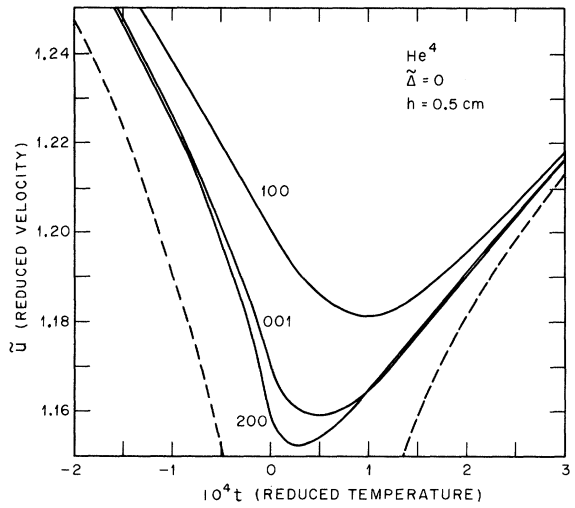

FIG. 18. Average dimensionless velocity $\tilde{u}$ along the critical isochore ($\tilde{\Delta}=0$) in He^4, plotted as a function of reduced temperature for various modes of the resonator. The dashed line represents the velocity out of gravity, which is the same for all modes. The modes are designated by the "quantum numbers" *pmn*, as explained in the text.

A total of 41 "data points" were calculated using $\alpha = 0.05$, by breaking up the interval $7\times10^{-5} \leq |t| \leq 7\times10^{-3}$ in logarithmic steps (this was done separately for $t>0$ and $t<0$). Least-square fits to the functional form used in the absence of gravity

$$C_v = (1+t)(A|t|^{-\alpha} + B_0) \qquad (6.1)$$

were made for the data in the interval $|t_{min}| \leq |t|$ $\leq |t_{max}|$, for different values of $|t_{min}|$, in order to find the best values of α (or α') and T_c. In Fig. 21, we show the best values of α and α', as a function of the corresponding value of $|t_{min}|$. (Unless otherwise noted, all values of t are referred to T_c^0.) We also show the shift in T_c [$\Delta t_c \equiv (T_c - T_c^0)/T_c^0$], and the normalized σ values, describing the quality of the fit for each case.

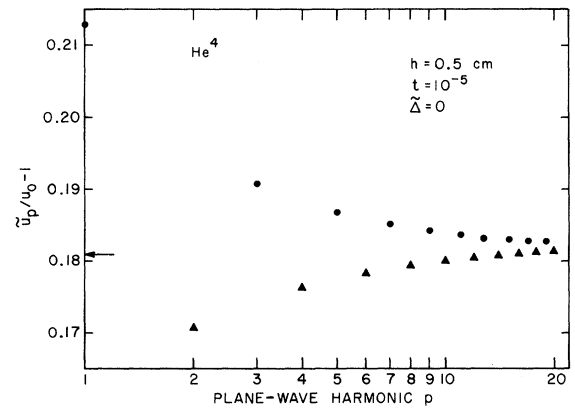

FIG. 19. Magnitude of the gravity correction $(\tilde{u}_p/u_0) - 1$ in He^4 at $t=10^{-5}$, $\tilde{\Delta}=0$, as a function of the "quantum number" p of the plane wave modes $\{p00\}$. The quantity $\tilde{u}_p$ is the average velocity in gravity and u_0 is its gravity-free value. The arrow represents the gravity correction for the Bessel function modes 001 and 010. Note that the largest gravity correction occurs for the fundamental plane-wave mode ($p=1$), and the smallest occurs for the second harmonic ($p=2$).

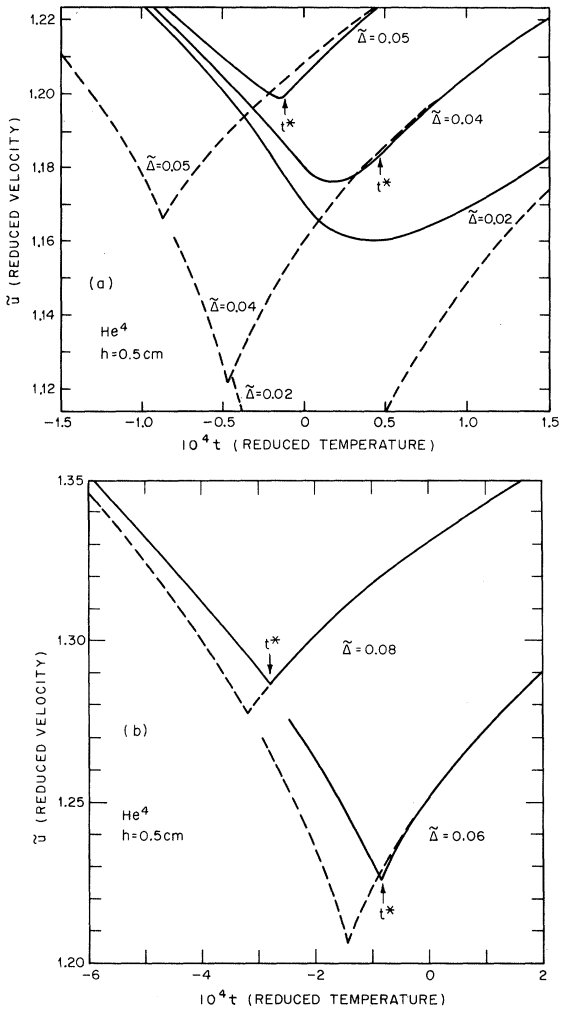

FIG. 20. Velocity in He^4 along the isochores $\tilde{\Delta}=0.02$, 0.04, and 0.05 [Fig. (a)] and $\tilde{\Delta}=0.06$ and 0.08 [Fig. (b)], plotted as a function of reduced temperature and expressed in dimensionless units. The dashed lines represent the velocity out of gravity, with a minimum and a cusp at the coexistence curve. For $\tilde{\Delta} < \tilde{\Delta}_0 = 0.048$, the velocity in gravity has a minimum which is below the characteristic temperature t^* (for $\tilde{\Delta}=0.02$ the value of $t^* = 2.3\times10^{-4}$ is outside the range of the figure). For $\tilde{\Delta} > \tilde{\Delta}_0^*$, the minimum occurs very near the temperature t^*.

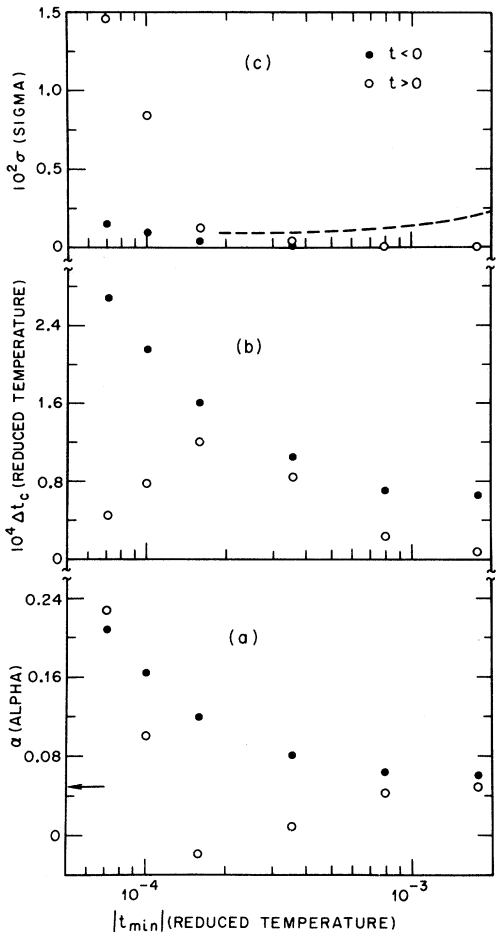

FIG. 21. Results of least-squares fits of the average specific heat for Xe with $h=1$ cm. Successive fits of the data in the interval $t_{min} \leq |t| \leq 7\times 10^{-3}$ were made for different values of t_{min}, with T_c and the exponents considered adjustable parameters. In (a), we show α and α' as a function of $|t_{min}|$. The starting values, in the absence of gravity, $\alpha=\alpha'=0.05$ are shown by an arrow. In (b) we show the deviation of the "best-fit" value of T_c from the true value T_c^0 [$\Delta t_c \equiv (T_c - T_c^0)/T_c^0$]. (c) contains the corresponding normalized σ values for each fit. These are obtained by dividing the standard deviation by the average of $\tilde{C}_v$ in the interval. The dashed line is an estimate of the minimum σ arising from realistic experimental data, due to scatter and correction terms.

terms, which we include in the fit. Thus our σ values for small intervals, which include primarily data points far from T_c, are unrealistically low. In practice, there is a minimum value for σ, which is roughly the percentage of scatter in the data. Moreover, points far from T_c will be more affected by correction terms, and if the number of points becomes too small, σ might be expected to rise due to poor statistics. We have indicated with a dotted line in Fig. 21(c), a more realistic estimate for the minimum σ, corresponding to an experimental accuracy of roughly 0.1%, and some reasonable correction terms. In these calculations we have treated T_c as separately adjustable for $t<0$ and $t>0$. From Fig. 21(b) we see that the T_c values determined in this manner are closest to each other for $|t_{min}| \approx 3.5\times 10^{-4}$. If we instead require that T_c be the same for $t>0$ and $t<0$, we find, for $|t_{min}| = 3.5\times 10^{-4}$, the values

$$\alpha = -0.001\,, \quad \alpha' = 0.0735\,, \quad \Delta t_c = 9.5\times 10^{-5}\,, \tag{6.2}$$

with a maximum gravity effect $\Delta C \equiv (\tilde{C}_v - C_v^0)/C_v^0 = 1.29\%$ at $t = +|t_{min}|$ and $\Delta C = -1.25\%$ at $t = -|t_{min}|$. For $|t_{min}| = 1.6\times 10^{-4}$ the corresponding numbers are

$$\alpha = -0.072\,, \quad \alpha' = 0.098\,, \quad \Delta t_c = 1.4\times 10^{-4}\,,$$
$$\Delta C = 11\% \text{ at } t = +|t_{min}|\,, \tag{6.2a}$$
$$\Delta C = -3.6\% \text{ at } t = -|t_{min}|\,.$$

From this analysis, a reasonable choice for α, α', and T_c would be that given in Eq. (6.2), which is to be compared to the ideal values $\alpha=\alpha'=0.05$, $\Delta t_c = 0$.

A different strategy is to fix T_c at the temperature of the specific-heat maximum, i.e., $\Delta t_c = -4.5\times 10^{-5}$. In that case, the α, α', and σ values are those shown in Fig. 22 and here we obtain, for $|t_{min}| = 3.5\times 10^{-4}$,

$$\alpha = 0.11\,, \quad \alpha' = -0.03\,, \quad \Delta t_c = -4.5\times 10^{-5}\,. \tag{6.3}$$

It is significant that when T_c is adjustable we find $\alpha' > \alpha$, whereas when T_c is fixed at the specific-heat maximum we have $\alpha' < \alpha$.

It is clear from the foregoing discussion that gravitational rounding of the specific heat can cause significant errors in the determination of the critical exponents. Similarly, in solids near magnetic critical points, there is considerable rounding of specific-heat singularities,[16,32] and we may expect errors in critical exponents which are comparable to or greater than those found here. In a fluid, of course, the rounding effects may be minimized by using thinner samples, so that more decades of temperature are available, in which both gravity effects and correction terms are unimportant. Such a strategy was employed in the recent measurements of Lipa, Edwards, and Buckingham,[22] which we shall briefly discuss.

B. Gravity Corrections for CO_2 with $h=0.1$ cm

We have calculated the gravity correction $\Delta C = (\tilde{C}_v - C_v^0)/C_v^0$ for CO_2 over the range $4\times 10^{-5} < |t| < 5\times 10^{-3}$ employed in Ref. 22, using their value for the height, $h=0.1$ cm. It must be noted that the form for C_v^0 which emerges from the "linear model" is quite different from the best fit found in Ref. 22,

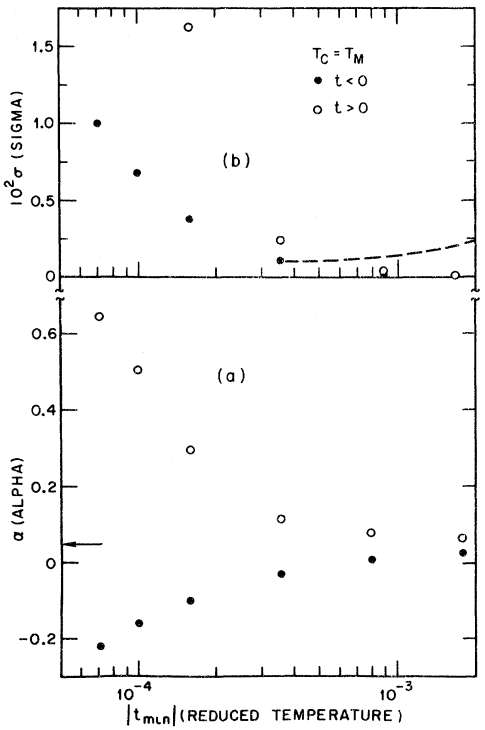

FIG. 22. Same analysis as in Fig. 20 is presented here, except that T_c is fixed at the temperature of the specific-heat maximum. Note that in contrast to Fig. 20, here we have $\alpha' < \alpha$.

since the linear model is not consistent with different values for B_0 and B_0' [see Eq. (2.6)] or with $\alpha = \frac{1}{8}$. Nevertheless, over the range of the fit, our function C_v^0 is numerically close to that of Ref. 22, and as shown in Sec. IV, the computed values of $(\tilde{C}_v - C_v^0)/C_v^0 \equiv \Delta C$ are rather insensitive to the form of C_v^0. In order to correct the data of Lipa *et al.* we have taken their best fit (in units of the gas constant R)

$$\tilde{C}_v^L/R = 5.583|t|^{-0.125} - 3.457\,, \quad t>0 \qquad (6.4a)$$

$$\tilde{C}_v^L/R = 10.473|t|^{-0.125} - 0.024\,, \quad t<0 \qquad (6.4b)$$

and have derived from it the "gravity-free" specific heat

$$(C_v^0)^L = \tilde{C}_v^L(1 - \Delta C)\,, \qquad (6.5)$$

using the computed values of ΔC. We find that the maximum gravity correction ΔC is 0.7% for $t>0$, and -0.9% for $t<0$. A least-squares fit to $(C_v^0)^L$ then yields

$$t>0: \quad \alpha = 0.135\,, \qquad \Delta t_c = 4.3\times10^{-6}\,; \qquad (6.6a)$$

$$t<0: \quad \alpha' = 0.120\,, \qquad \Delta t_c = 4.2\times10^{-6}\,. \qquad (6.6b)$$

In this case the shifts in α and T_c are just within the uncertainties quoted in Ref. 22. It is interesting to note, however, that the difference $B_0' - B_0$ [see Eq. (2.6c)] is reduced from 3.43 to 1.67.

C. Exponent β Derived from Apparent Coexistence Curve

Given an apparent coexistence curve with a flat top, as shown in Fig. 6, it is difficult to assign a meaningful apparent value for β. Nevertheless, for sufficiently small values of h, the flat portion is never actually observed, since it is smeared by experimental uncertainties in the temperature. For instance, for $h = 0.1$ cm in Xe, an uncertainty in t of $\pm10^{-6}$ near $t=0$, leads to a spread of Δ^* of ±0.035, which is just the width of the flat portion of $\tilde{\Delta}^*(t)$. Accordingly, we have chosen as our "data," points on the curve $\tilde{\Delta}^*(t)$ for $h = 0.1$ cm, between $t = -10^{-6}$ and $t = -1.25\times10^{-3}$. We have fitted these "data" to the form

$$\tilde{\Delta}^*(t) = B[(T_c - T)/T_c]^{\beta}\,, \qquad (6.7)$$

with B, β, and T_c adjustable. Once again points were chosen on a logarithmic scale, and successive portions nearest T_c^0 were discarded, in an effort to find the best values of T_c and β. The results are shown in Table IV, from which we see that with $t_{min} = -3\times10^{-5}$ we obtain $\beta = 0.359$, with a normalized σ of 0.013, which is close to the minimum expected with real experimental data. The values of β are to be contrasted to the "ideal" value $\beta = 0.351$. The prefactor B deviates significantly from its "ideal" value in all cases. From the above analysis it seems clear that gravity can easily introduce errors in β of ±0.005.

For capacitance measurements of the coexistence curve, the effective height may be much less than $h = 0.1$ cm, but the total height of the sample is often much larger, and the thermodynamic path followed by the portion under investigation might be quite complicated. Very recently, a careful analysis of the coexistence curve of CO_2, N_2O, and $CClF_3$ was made by Levelt Sengers, Straub, and Vicentini-Missoni.[33] The experimental data for this study were those of Schmidt and of Straub,[34] obtained by using the gravity effect explicitly, and presumably the effects we discuss here would not be present in those measurements.

VII. SUMMARY AND CONCLUSION

In this paper we have presented detailed quantitative estimates of the effect of gravity at the gas-liquid critical point, based on the "linear-model" parametric equation of state. This equation is sufficiently simple to allow a convenient analysis at arbitrary points in the (ρ, T) plane. On the other hand, we believe that it is realistic enough so that the main uncertainties in our analysis are due to errors in the PVT measurements which determine the parameters, rather than in the equation of state itself.

TABLE IV. Least-squares fit to apparent coexistence curve. The fits were made in the intervals $t_{\min} \geq t \geq -1.25\times 10^{-3}$. Xe, $h=0.1$ cm. Gravity-free values: $\beta=0.351$, $B=1.795$.

$t_{\min}$	Δt_c	β	B	σ	$(\Delta^* - \Delta_L)$ at $t=t_{\min}$	$(\Delta^* - \Delta_L)/\Delta_L$ at $t=t_{\min}$
-10^{-6}	1.5×10^{-5}	0.367	2.20	4×10^{-2}	0.021	1.50
-3×10^{-5}	1.1×10^{-5}	0.359	2.08	1.3×10^{-2}	0.004	0.09
-3×10^{-4}	5×10^{-6}	0.352	1.99	5.5×10^{-3}	0.0003	0.003
-7×10^{-4}	4×10^{-6}	0.352	1.98	2.7×10^{-3}	0.0001	0.0007

The physical quantities we have calculated are the local density distribution in a sample of given average density, the average specific heat, and the average sound velocity. We conclude that except possibly for a few recent cases, the effect of gravity leads to important quantitative corrections to the critical exponents. These corrections can be made reliably, however, using the methods presented here.

ACKNOWLEDGMENTS

We wish to thank Mrs. A. B. Kane and Miss J. Seery for assistance in the numerical computations. We are also indebted to Dr. E. Wasserstrom for the solution of the wave equation presented in Sec. V.

APPENDIX A

Parametric Representation

The parametric variable r and θ are defined in Eqs. (2.1)–(2.2) in the text, and the scaled equation of state in terms of these variables is relation (2.3a). The simple form of Eq. (2.3a) permits a direct integration of Eq. (2.4) for the free energy $A(\rho, T)$ which yields

$$A(\rho, T) = A_s(\rho, T) + \mu_0(T)\rho + A_0(T) , \tag{A1}$$

where $A_0(T)$ and $\mu_0(T) \equiv \mu(\rho_c, T)$ are assumed to be analytic functions of T near T_c. An explicit expression for $A_s(\rho, T)$ in terms of the variables r and θ is given in Eqs. (A2)–(A4) below. From this expression we may obtain all the other thermodynamic functions by differentiation. Before doing this, let us introduce a convenient set of dimensionless units.

Dimensionless Units

We express the free energy and the pressure in units of P_c, the temperature in units of T_c, the density in units of ρ_c, and the chemical potential in units of P_c/ρ_c. It follows that $A(\rho, T)$ is a free energy per unit volume, and the entropy will also be per unit volume (in units of P_c/T_c). The specific heat per unit mass is $C_v = \rho^{-1}T(\partial S/\partial T)_\rho$, and is expressed in units of $P_c/T_c\rho_c$. In order to obtain the specific heat per mole, one multiplies the dimensionless specific heat by $C_N = (P_c w/T_c\rho_c)\times 10^{-7}$ J/mole °K; w is the molecular weight. Similarly, the dimensionless sound velocity must be multiplied by $U_N = (P_c/\rho_c)^{1/2}$ to obtain its dimensional value in units of cm/sec. Finally, the dimensionless coordinate z is expressed in terms of the sample height h.

Thermodynamic Functions

The integral of Eq. (2.4) yields Eq. (A1) with

$$A_s = f(\theta) r^{\beta(\delta+1)} = f(\theta) r^{2-\alpha} , \tag{A2}$$

$$f(\theta) = f_0 + f_2\theta^2 + f_4\theta^4 , \tag{A3}$$

$$f_0 = (ak/2b^4)[\delta - 3 - b^2\alpha(\delta-1)][(\delta+1)(\alpha-1)\alpha]^{-1} , \tag{A4a}$$

$$f_2 = -(ak/2b^2)[\beta(\delta-3) - b^2\alpha(1-2\beta)][\alpha(\alpha-1)]^{-1} , \tag{A4b}$$

$$f_4 = -\tfrac{1}{2} ak(1-2\beta)\alpha^{-1} . \tag{A4c}$$

The critical exponents satisfy the usual scaling relations,[10] $\beta(\delta+1) = 2-\alpha = \gamma + 2\beta$.

The entropy $S = -(\partial A/\partial T)_\rho$ is given by

$$S(\rho, T) = -A_0' - \rho\mu_0' + S_s , \tag{A5}$$

where

$$S_s(r, \theta) = s(\theta) r^{1-\alpha} , \tag{A6}$$

$$s(\theta) = -\beta[1 - b^2(1-2\beta)\theta^2]^{-1} \times [(\delta+1) f_0 + (\delta-1) f_2\theta^2 + (\delta-3) f_4\theta^4] , \tag{A7a}$$

and the primes in Eq. (A5) denote differentiation with respect to T. This last expression may be simplified,[34a] using Eqs. (A4) and the scaling relations between exponents, to read

$$s(\theta) = L_0(\bar{s}_0 + \bar{s}_2\theta^2) , \tag{A7b}$$

with

$$L_0 = ak/[2b^4\alpha(1-\alpha)] , \tag{A7c}$$

$$\bar{s}_0 = \beta(\delta-3) - b^2\beta\alpha(\delta-1) , \tag{A7d}$$

$$\bar{s}_2 = (\alpha-1)(\delta-3)\beta b^2 . \tag{A7e}$$

The specific heat $C_v = \rho^{-1}T(\partial S/\partial T)_\rho$ is

$$C_v = C_v^{\text{sing}} + C_v^B , \tag{A8}$$

with

$$C_v^B = [(1+t)/(1+\Delta)][-A_0'' - (1+\Delta)\mu_0'']\,, \quad \text{(A9)}$$

$$\Delta = k\theta r^{\beta}\,, \quad \text{(A10)}$$

$$C_v^{\text{sing}} = [(1+t)/(1+\Delta)]c_m(\theta)r^{-\alpha}\,, \quad \text{(A11)}$$

and

$$c_m(\theta) = -\beta(1-d^2\theta^2)^{-3}(a_1a_2 - a_3)\,, \quad \text{(A12a)}$$

where

$$a_1 = [(1-d^2\theta^2)(1-\alpha) - 2d^2\beta\theta^2]\,, \quad \text{(A12b)}$$

$$a_2 = [(\delta+1)f_0 + (\delta-1)f_2\theta^2 + (\delta-3)f_4\theta^4]\,, \quad \text{(A12c)}$$

$$a_3 = \{2\beta\theta^2(1-d^2\theta^2)[(\delta-1)f_2 + 2(\delta-3)f_4\theta^2]\}, \quad \text{(A12d)}$$

$$d^2 = b^2(1-2\beta)\,. \quad \text{(A13)}$$

A simpler expression for $c_m(\theta)$ may be obtained directly from Eq. (A7b)

$$c_m(\theta) = L_0(1-d^2\theta^2)^{-1}[(1-\alpha)\bar{s}_0 + (1-\alpha-2\beta)\bar{s}_2\theta^2] \quad \text{(A13a)}$$

In order for the specific heat to remain finite away from the critical point (i.e., for $r \neq 0$) we must have

$$b^2(1-2\beta) < 1\,. \quad \text{(A14)}$$

The specific heat at constant chemical potential $C_\mu = \rho^{-1}T(\partial S/\partial T)_\mu$ is given by

$$C_\mu = C_v + T\left(\frac{\partial S}{\partial \rho}\right)_T\left(\frac{\partial \rho}{\partial T}\right)_\mu \equiv C_\mu^B + C_\mu^{\text{sing}}\,. \quad \text{(A15)}$$

The "background" contribution is

$$C_\mu^B = C_v^B - \left(\frac{1+t}{1+\Delta}\right)\mu_0'\left(\frac{\partial \rho}{\partial T}\right)_\mu\,, \quad \text{(A16)}$$

and the singular term is

$$C_\mu^{\text{sing}} = [(1+t)/(1+\Delta)]c_h(\theta)r^{-\alpha}\,, \quad \text{(A17)}$$

where

$$c_h(\theta) = \beta(c_1 + c_2)/c_3\,, \quad \text{(A18a)}$$

with

$$c_1 = (\alpha-1)(1-3\theta^2)(1-d^2\theta^2)[(\delta+1)f_0 + (\delta-1)f_2\theta^2 + (\delta-3)f_4\theta^4]\,, \quad \text{(A18b)}$$

$$c_2 = 2\beta\delta\theta^2(1-\theta^2)[d^2(\delta+1)f_0 + (\delta-1)f_2 + (\delta-3)f_4\theta^2(2-d^2\theta^2)]\,, \quad \text{(A18c)}$$

$$c_3 = (1-d^2\theta^2)^2[1 + (2b^2\beta\delta - 3 - b^2)\theta^2 - b^2(2\beta\delta-3)\theta^4]\,. \quad \text{(A18d)}$$

As in the case of C_v, a simplified expression[34a] may be obtained directly from Eq. (A7), namely,

$$c_h(\theta) = L_0\left(\frac{(1-\alpha)(1-3\theta^2)(\bar{s}_0 + \bar{s}_2\theta^2) - 2\beta\delta\theta^2\bar{s}_2(1-\theta^2)}{1 + (2b^2\beta\delta - 3 - b^2)\theta^2 - b^2(2\beta\delta-3)\theta^4}\right)\,. \quad \text{(A18e)}$$

The compressibility κ_T is given by

$$\left(\frac{\partial \mu}{\partial \rho}\right)_T = (\rho^2\kappa_T)^{-1} = \frac{a}{k}r^{\gamma}\chi(\theta)\,, \quad \text{(A19)}$$

where

$$\chi(\theta) = \{1 - [3 + b^2(1-2\beta\delta)]\theta^2 + b^2\theta^4(3-2\beta\delta)\} \times (1-d^2\theta^2)^{-1}\,. \quad \text{(A20)}$$

In order to calculate the sound velocity we also need $(\partial P/\partial T)_\rho$, which is given by

$$\left(\frac{\partial P}{\partial T}\right)_\rho = -A_0' + S + (1+\Delta)p(\theta)r^{\beta\delta-1}\,, \quad \text{(A21)}$$

with

$$p(\theta) = a\beta\theta[(\delta-1) + (3-\delta)\theta^2](1-d^2\theta^2)^{-1}\,. \quad \text{(A22)}$$

The adiabatic sound velocity u is then obtained from the relation

$$u^2 = (\rho\kappa_T)^{-1} + T\left(\frac{\partial P}{\partial T}\right)_\rho^2(\rho^2 C_v)^{-1}\,. \quad \text{(A23)}$$

As was pointed out in Ref. 12, use of the "minimization" condition (2.5) simplifies the thermodynamic expressions further. In particular, $c_m(\theta)$ becomes independent of θ,

$$c_m(\theta) = ak\gamma^2(\gamma-1)(1-2\beta)/[2\alpha(\gamma-2\beta)]\,, \quad \text{(A24)}$$

and Eqs. (A20) and (A22) are changed to

$$\chi(\theta) = 1 + [(2\beta\delta-3)/(1-2\beta)]\theta^2 \quad \text{(A25)}$$

and

$$p(\theta) = a\beta(\delta-1)\theta\,. \quad \text{(A26)}$$

APPENDIX B

Determination of "Linear-Model" Parameters

The parameters a and k in Eqs. (2.1) and (2.3a) are determined from experimental data on the shape of the coexistence curve

$$(\rho_L - \rho_c)/\rho_c \equiv \Delta_L(t) = B(-t)^{\beta} \quad \text{(coexistence curve)}\,, \quad \text{(B1)}$$

and the compressibility on the critical isochore for $t > 0$,

$$\kappa_T = \Gamma t^{-\gamma}\,, \quad \rho = \rho_c\,, \quad t > 0 \quad \text{(B2)}$$

(note that κ_T is expressed in units of P_c^{-1}, see Appendix A). Comparing Eq. (B1) with Eq. (2.3a) for $\theta = 1$ we obtain

$$k = B(b^2 - 1)^{\beta}, \tag{B3}$$

and comparing Eq. (B2) with Eq. (A19) for $\theta = 0$, we find

$$a = k/\Gamma. \tag{B4}$$

In order to determine b we can use either the shape of the critical isotherm

$$\Delta\mu = D\Delta|\Delta|^{\delta-1}, \quad t > 0 \tag{B5}$$

or the ratio Γ/Γ', where Γ' is defined by[10]

$$\kappa_T = \Gamma'(-t)^{-\gamma}, \quad \rho = \rho_c, \quad t < 0. \tag{B6}$$

It follows from Eqs. (2.1), (2.3a), (A19), (A20), (B5), and (B6) that

$$D = ab^{\delta-3}k^{-\delta}(b^2 - 1), \tag{B7}$$

$$\Gamma/\Gamma' = 2(b^2 - 1)^{1-\gamma}[1 - b^2(1 - 2\beta)]^{-1}. \tag{B8}$$

As noted in Sec. II, in view of the uncertainties in the experimental values of D, B, Γ, and Γ', we may in practice use a different criterion than Eqs. (B7) and (B8) to determine b, namely, the "minimization" condition (2.5). In any case b^2 must satisfy the inequalities [cf. Eqs. (2.2a) and (A14)]

$$b^2(1 - 2\beta) < 1, \quad b^2 > 1. \tag{B9}$$

In Figs. 15(b) and 15(c) we show the dependence of D and Γ/Γ', determined from Eqs. (B7) and (B8), respectively, on the value of b^2. It is seen that a range of values of b^2, other than that determined by Eq. (2.5), are consistent with experiment at the present time. The only other quantities which are necessary for a full specification of the thermodynamics in our model are the functions $A_0(T)$ and $\mu_0(T)$ of Eq. (A1). Since these functions are assumed to be analytic, we can expand them in power series about T_c. We shall retain the constants $A_0'(T_c)$, $A_0''(T_c)$, and $\mu_0''(T_c)$, which we determine by fitting to experimental data, where possible. The quantity $A_0''(T_c) + \mu_0''(T_c)$ is fixed by the value of the specific heat on the critical isochore far from T_c (say at $t = 10^{-3}$), and $\mu_0''(T_c)$ is obtained from the asymmetry of C_v about $\rho = \rho_c$, at fixed t, far from T_c. Finally, the constant $A_0'(T_c)$ is determined from the value of $(\partial P/\partial T)_\rho$ at $T = T_c$ (see Table I).

In Ref. 15, it was misleadingly stated that the "linear model" forced us to choose the value $\alpha = 0.05 \pm 0.02$ for xenon. This was because, given the experimental values of β, B, and Γ, the quantity $C_v(-t) - C_v(t)$ depends only on α, and can therefore be accurately fitted to experiment far from T_c, thus determining α. As pointed out by Schmidt,[9] however, there is in practice enough uncertainty in β, B, and Γ, that α is not accurately determined by such a fit. Nevertheless, it is important to note that there exists a *correlation* in the "linear model" between the exponent α, and the values of β, B, and Γ. This correlation is almost certainly spurious, since it is a consequence of the questionable assumption that there are no singular corrections to the asymptotic behavior of C_v. In terms of Eq. (2.6), this is the assumption $B_0 = B_0'$, which has also been made in other explicit model equations of state.[10,11] As mentioned earlier, it is inconsistent to assume $B_0 \neq B_0'$ in the specific heat, and to neglect singular correction terms in other thermodynamic functions. From Eq. (2.6) we may write

$$C_v(-t) - C_v(t) = (A' - A)|t|^{-\alpha} + (B_0' - B_0), \tag{B10}$$

and for given β, B, and Γ, the first term in Eq. (B10) depends only on α. If $B_0 = B_0'$, then as mentioned previously, the measured difference in C_v determines α, once β, B, and Γ are known. A similar fit can be carried out with other explicit equations of state containing regular correction terms.[10,11] In reality, however, the correction terms are probably not regular ($B_0 \neq B_0'$),[22,23] and the correlation between β, B, Γ, and α is spurious. Even within the linear model, the statement made in Ref. 15 that $\alpha = 0.05 \pm 0.01$, referred only to the specific values $\beta = 0.351$, $B = 1.795$, $\Gamma = 0.049$. Taking into account the uncertainties in these quantities we find, rather, that from a fit of $C_v(-t) - C_v(+t)$ to experiment at $t = \pm 10^{-3}$ (see Table III), the linear model yields $\alpha = 0.065 \pm 0.02$, which is similar to Schmidt's[9] analysis based on the equation of state of Ref. 11.

In Table I, we show values for the parameters of the linear model in a number of pure fluids. Whenever specific-heat data were available we have chosen β from PVT measurements and then fitted α to the specific-heat difference at $t = 10^{-3}$, as discussed above. In the absence of specific-heat data, we have taken β and δ from PVT measurements, and determined α by the relation $\alpha = 2 - \beta(\delta + 1)$. The constants A_0'' and μ_0'' have been fitted to specific-heat data at $t \gtrsim 10^{-3}$. Some of the uncertainties in the "linear-model" parameters are shown for Xe in Table III; these result from uncertainties in β, Γ, and B.

APPENDIX C

Coordinates of Top and Bottom of the Vessel

As explained in Sec. III, the coordinate z_1 of the bottom of the vessel is determined, for given values of t and $\tilde{\Delta}$, by the solution of the equation

$$\tilde{\Delta} = \int_{z_1}^{1+z_1} \Delta(t, z)\, dz, \tag{C1}$$

where

$$\Delta(t, z) = k\theta(t, z)[r(\theta)]^{\beta}, \tag{C2}$$

and $\theta(t, z)$ is the inverse of the function [cf. Eq. (3.7)]

$$z(t, \theta) = -x_1\theta(1-\theta^2)r^{\beta\delta}, \tag{C3}$$

with

$$r(\theta) = t(1-b^2\theta^2)^{-1}. \tag{C4}$$

Let us transform Eq. (C1) to a θ integral and define

$$H(\theta_1) \equiv \tilde{\Delta} + \int_{\theta_1}^{\theta_2} g(\theta)\, d\theta, \tag{C5}$$

$$g(\theta) = x_1 k t^{-1}\theta\,[r(\theta)]^{3-\alpha}\{1+[(2\beta\delta-1)b^2-3]\theta^2 + b^2(3-2\beta\delta)\theta^4\}, \tag{C6}$$

where

$$\theta_1 = \theta(z_1), \tag{C7}$$

$$\theta_2(\theta_1) = \theta[1+z(\theta_1)]. \tag{C8}$$

We wish to find the zero of the function $H(\theta_1)$, which we do by employing Newton's method.[35] For each choice of θ_1 we calculate $\theta_2(\theta_1)$ numerically, from Eq. (C8) and its inverse, and then perform the integral in Eq. (C5) to find $H(\theta_1)$. The derivative $H'(\theta_1)$, which is needed for Newton's method,[35] can be shown to be equal to

$$H'(\theta_1) = \left[\left(\frac{\partial z}{\partial\theta}\right)_{\theta=\theta_1} \Big/ \left(\frac{\partial z}{\partial\theta}\right)_{\theta=\theta_2}\right] g(\theta_2) - g(\theta_1), \tag{C9}$$

with

$$\frac{\partial z}{\partial\theta} = -t^{-1}x_1[r(\theta)]^{1+\beta\delta}\{1+[(2\beta\delta-1)b^2-3]\theta^2 + b^2(3-2\beta\delta)\theta^4\}. \tag{C10}$$

We have found that in most cases Newton's method converges in five or six attempts. Given the value of θ_1, the coordinate is determined using Eq. (C3) as

$$z_1 = z(\theta_1). \tag{C11}$$

Special Cases

1. Critical Isochore ($\tilde{\Delta}=0$)

When the average density is the critical density, the integral in Eq. (C1) must be zero, and since the integrand is odd we have

$$z_1 = -(1+z_1) = -\tfrac{1}{2}, \tag{C12}$$

$$\theta_1 = \theta(-\tfrac{1}{2}) = -\theta(\tfrac{1}{2}). \tag{C13}$$

In this case the point of maximum density gradient, which is the gas-liquid interface for $t<0$, is always in the center of the vessel. This fact is of course a consequence of the symmetry assumptions we have made in the equation of state.

2. Critical Isotherm ($t=0$)

On the critical isotherm we have

$$\theta = b^{-1}\,\mathrm{sgn}\Delta, \tag{C14}$$

and Eqs. (C4)–(C6) simplify considerably. We have

$$|\Delta| = kb^{-1}r^{\beta}, \tag{C15}$$

$$z = -x_1(\mathrm{sgn}\,\Delta)\,b^{-1}(1-b^{-2})r^{\beta\delta}, \tag{C16}$$

so Eq. (C5) can be integrated to yield

$$\tilde{\Delta}_0 = -\tilde{\Delta}_0^*\{|1+z_1|^{1+\delta^{-1}} - |z_1|^{1+\delta^{-1}}\}, \tag{C17}$$

where

$$\tilde{\Delta}_0^* = kb^{-1}(1+\delta^{-1})^{-1}[b^{-1}(1-b^{-2})x_1]^{-1/\delta}. \tag{C18}$$

It is a simple matter to solve Eq. (C17) numerically for z_1 as a function of $\tilde{\Delta}$.

3. Limit of Zero Gravity

This limit is attained when the height h vanishes, i.e., when x_1 [Eq. (3.8)] becomes large. More precisely, the criterion for negligible gravity effect at $\tilde{\rho}=\rho_c$ is

$$x_1^{1/\beta\delta}|t| \gg 1. \tag{C19}$$

In that case, it can be seen from Eq. (C10) that $(\partial z/\partial\theta) \gg 1$, so θ remains essentially constant over the range $\Delta z = 1$. The value θ_0 of θ can be found by taking $\Delta(z)$ out of the integrand in Eq. (C1), i.e.,

$$\tilde{\Delta} = \Delta[z(\theta_0)] = k\theta_0[r(\theta_0)]^{\beta}, \tag{C20}$$

which can be solved (numerically) for $\theta_0(\tilde{\Delta}, t)$.

The above result holds in the one-phase region,

$$|\tilde{\Delta}| > \Delta_L(t) = B(-t)^{\beta}, \tag{C21}$$

with $B = k(b^2-1)^{-\beta}$. In the two-phase region,

$$|\tilde{\Delta}| \le \Delta_L(t), \tag{C22}$$

we have

$$\tilde{\Delta} = (1+z_1)\Delta_G(t) - z_1\Delta_L(t), \tag{C23}$$

where $\Delta_G(t) = -\Delta_L(t)$. Clearly the solution of Eq. (C7) in the absence of gravity is $\theta_1 = \theta_0^{(1)} = +1$ for $z = z_1$ and $\theta_2 = \theta_0^{(2)} = -1$ for $z = 1+z_1$, and the quantity $-z_1$ represents the (volume) fraction of liquid. When $z_1 = 0$, the interface is at the bottom and there is no liquid, and when $z_1 = -1$ the interface is at the top and the system is entirely liquid.

APPENDIX D

Average Specific Heat

From Eqs. (4.1) and (4.2) we see that the singular part of the average specific heat is proportional to

$$\tilde{S}' = \frac{d}{dt}\int_{z_1}^{1+z_1} S_s(t, z)\, dz, \tag{D1}$$

where the function $S_s(t, z)$ is obtained from $S_s(\theta, r)$ [Eq. (A6)], by expressing θ and r as functions of z.[36] Carrying out the differentiation in Eq. (D1) we find

$$\tilde{S}' = \int_{z_1}^{1+z_1} \frac{\partial}{\partial t} S_s(t, z)\, dz - \left(\frac{\partial z_1}{\partial t}\right)_{\tilde{\Delta}} [S_s(t, z_1) - S_s(t, 1+z_1)]. \quad \text{(D2)}$$

Next, differentiate Eq. (C1),

$$0 = \int_{z_1}^{1+z_1} \frac{\partial \Delta(t, z)}{\partial t}\, dz + \left(\frac{\partial z_1}{\partial t}\right)_{\tilde{\Delta}} [\Delta(t, 1+z_1) - \Delta(t, z_1)], \quad \text{(D3)}$$

which yields

$$\tilde{S}' = \int_{z_1}^{1+z_1} \frac{\partial}{\partial t} S_s(t, z)\, dz - \left(\frac{S_s(t, 1+z_1) - S_s(t, z_1)}{\Delta(t, 1+z_1) - \Delta(t, z_1)}\right) \int_{z_1}^{1+z_1} \frac{\partial}{\partial t} \Delta(t, z)\, dz. \quad \text{(D4)}$$

The integrals in Eq. (D4) are most conveniently carried out in the θ variable. Using the relationship between z and θ given in Eqs. (C3) and (C4), we find by a tedious but straightforward calculation

$$\tilde{S}' = \int_{\theta_1}^{\theta_2} \Sigma_1(t, \theta)\, d\theta - \left(\frac{S_s(t, \theta_2) - S_s(t, \theta_1)}{\Delta(t, \theta_2) - \Delta(t, \theta_1)}\right) \int_{\theta_1}^{\theta_2} \Sigma_2(t, \theta)\, d\theta, \quad \text{(D5)}$$

where[34a]

$$\Sigma_1(t, \theta) = t^{-1} x_1 \beta (1 - d^2\theta^2)^{-1} r^{\beta\delta+1-\alpha} [f_0(\delta+1) + f_2(\delta-1)\theta^2 + f_4(\delta-3)\theta^4] \times \left[(1-\alpha)(1-3\theta^2) - 2\beta\delta\theta^2(1-\theta^2)\left(\frac{d^2}{1-d^2\theta^2} + \frac{(\delta-1)f_2 + 2(\delta-3)f_4\theta^2}{f_0(\delta+1) + f_2(\delta-1)\theta^2 + f_4(\delta-3)\theta^4}\right)\right], \quad \text{(D6)}$$

$$\Sigma_2 = -k\beta t^{-1} x_1 r^{2-\alpha} \theta [1 - \delta + (\delta-3)\theta^2], \quad \text{(D7)}$$

and r is here considered a function of θ and t, given in Eq. (C4).

Although the expressions in Eqs. (D5)–(D7) are cumbersome to write down, they may be evaluated quite simply on the computer, and the integrals in Eq. (D5) carried out. Since the integrand is not smooth near $t = 0$, we have changed to the variable

$$y = (x_0 t)^{-1}(1 - b|\theta|), \quad \text{(D8)}$$

which leads to well-behaved integrals.

The "background" contribution $\tilde{C}_v^B$ [see Eqs. (A9) and (A16)] is assumed to have its gravity-free value, which differs in the one-phase and two-phase regions. In the one-phase region [Eq. (C21)] we have [cf. Eq. (A9)]

$$\tilde{C}_v^B = [(1+t)/(1+\tilde{\Delta})][-A_0'' - (1+\tilde{\Delta})\mu_0''], \quad \text{(D9)}$$

whereas in the two-phase region we have [cf. Eq. (A16) and Ref. 28]

$$\tilde{C}_v^B = \left(\frac{1+t}{1+\tilde{\Delta}}\right)\left[-A_0'' - (1+\tilde{\Delta})\mu_0'' - (1+\tilde{\Delta})\mu_0'\left(\frac{\partial \Delta_L}{\partial t}\right)\left(\frac{\tilde{\Delta}}{\Delta_L(1+\tilde{\Delta})}\right)\right]. \quad \text{(D10)}$$

Special Cases

1. Limit of Zero Gravity

In this case θ is constant over the height of the specimen [see Appendix C], and we may write Eq. (D5) as

$$\tilde{S}' = \left.\frac{\partial S}{\partial t}\right|_{z, \theta=\theta_0} - \left.\frac{\partial S}{\partial \Delta}\right|_{t, \theta=\theta_0} \times \left.\frac{\partial \Delta}{\partial t}\right|_{z, \theta=\theta_0}. \quad \text{(D11)}$$

Since z is proportional to μ [Eq. (3.5)], we have

$$\tilde{S}' = \left.\frac{\partial S}{\partial t}\right|_{\mu} - \left.\frac{\partial S}{\partial \Delta}\right|_{t} \times \left.\frac{\partial \Delta}{\partial t}\right|_{\mu}, \quad \text{(D12)}$$

or in dimensional units,

$$T\tilde{S}' = T\left.\frac{\partial S}{\partial T}\right|_{\mu} - T\left.\frac{\partial S}{\partial \rho}\right|_{T} \times \left.\frac{\partial \rho}{\partial T}\right|_{\mu}, \qquad T\tilde{S}' = \rho C_\mu^0 + \frac{T}{\rho\kappa_T}\left(\frac{\partial \rho}{\partial T}\right)_\mu^2 = \rho C_v^0, \quad \text{(D13)}$$

i.e., the average specific heat indeed reduces to C_v^0. The above results holds for the one-phase region, $|\tilde{\Delta}| > \Delta_L(t)$. For the two-phase region, it was shown in Appendix C that $\theta_1 = 1$ and $\theta_2 = -1$. An inspection of Eqs. (D5) and (D7) shows that the second integral in Eq. (D5) vanishes by symmetry, and we are left with the first integral, which in the

present case is

$$\tilde{S}' = (\rho/T)C_\mu^0 . \tag{D14}$$

Thus, in the two-phase region the "constant-volume" specific heat reduces to the correct quantity[28] which is the average of C_μ^0 for the gas and the liquid (in our model the two are equal).

2. Critical Isochore ($\tilde{\Delta} = 0$)

In this case we have

$$z_1 = -\tfrac{1}{2} , \tag{D15}$$

$$\theta_1 = -\theta_2 = \theta(-\tfrac{1}{2}) \tag{D16}$$

for all values of t, and only the first term in Eq. (D5) contributes, due to the oddness of Σ_2.

3. Critical Isotherm ($t = 0$)

On the critical isotherm the gravity average of the specific heat can be carried out explicitly and the resulting expressions written down in closed form, as a function of density. The coordinate $z_1(\tilde{\Delta})$ is given by the solution of Eq. (C17). It is then more convenient to write the integrals in Eq. (D5) in terms of the variable

$$r(z) = [\,|z|\, x_1^{-1} b(1-b^{-2})^{-1}\,]^{1/\beta\delta} , \tag{D17}$$

since the integrals can be carried out explicitly. The answer is

$$\tilde{S}' = \tilde{S}_1' + \tilde{S}_2' , \quad t = 0 \tag{D18}$$

where[34a]

$$\tilde{S}_1' = K_1 x_1^{\alpha/\beta\delta}[\mathrm{sgn}(1+z_1)\,|1+z_1|^{1-\alpha/\beta\delta} - \mathrm{sgn}(z_1)\,|z_1|^{1-\alpha/\beta\delta}] , \tag{D19}$$

$$\tilde{S}_2' = K_2 x_1^{(1-\beta)/\beta\delta}\left(\frac{S_s(1)-S_s(2)}{\mathrm{sgn}(z_1)\Delta(1) - \mathrm{sgn}(1+z_1)\Delta(2)}\right)(|1+z_1|^{(1-\alpha)/\beta\delta} - |z_1|^{(1-\alpha)/\beta\delta}) , \tag{D20}$$

$$K_1 = [b^{-1}(1-b^{-2})]^{-1+\alpha/\beta\delta} s_0 [4b(\beta\delta-\alpha)]^{-1} \times\left[(1-\alpha)(1-3b^{-2}) - 2\beta\delta b^{-2}(1-b^{-2})\left(\frac{b^2(1-2\beta)}{2\beta} + 2s_0^{-1}(\delta-3)f_4 b^{-2} + s_0^{-1}(\delta-1)f_2\right)\right] , \tag{D21}$$

$$K_2 = \left(\frac{k\beta}{2b^2(\alpha-1)}\right)[1-\delta+b^{-2}(\delta-3)]\,[b^{-1}(1-b^{-2})]^{(\alpha-1)/\beta\delta} , \tag{D22}$$

$$S_s(1) = -\tfrac{1}{2} s_0 [r(z_1)]^{1-\alpha} , \tag{D23}$$

$$S_s(2) = -\tfrac{1}{2} s_0 [r(1+z_1)]^{1-\alpha} , \tag{D24}$$

$$\Delta(1) = kb^{-1}[r(z_1)]^\beta , \tag{D25}$$

$$\Delta(2) = kb^{-1}[r(1+z_1)]^\beta , \tag{D26}$$

$$s_0 = (\delta-3)f_4 b^{-4} + (\delta-1)f_2 b^{-2} + (\delta+1)f_0 , \tag{D27}$$

and $r(z)$ is defined in Eq. (D17).

We note that for $\tilde{\Delta} = 0$, $z_1 = -\frac{1}{2}$, and $\tilde{S}_2' = 0$, so

$$\tilde{S}' = (2x_1)^{\alpha/\beta\delta} K_1 , \quad \tilde{\Delta} = 0 , \quad t = 0 . \tag{D28}$$

Since K_1 is a pure number [cf., Eq. (D21)], we have $\tilde{C}_v \propto h^{-\alpha/\beta\delta}$ at $t = 0$, $\tilde{\Delta} = 0$. Thus on the critical isotherm the gravity average of the specific heat can be carried out explicitly, and the resulting expression written down in closed form, for arbitrary density.

APPENDIX E

Solution of Wave Equation

We wish to find the solution of Eq. (5.2),

$$\nabla^2\Phi(\vec{r}', \tau) - u^{-2}(z)\left(\frac{\partial^2}{\partial\tau^2}\right)\Phi(\vec{r}', \tau) = 0 , \tag{5.2}$$

with the boundary condition

$$\vec{\nabla}\Phi = 0 , \quad r' = a' , \quad z = z_1 , \quad 1+z_1 . \tag{5.3}$$

Let us set

$$\Phi(\vec{r}', \tau) = J_m(Ar')(\cos m\varphi) f(z) e^{-i\omega\tau} , \tag{E1}$$

where r', φ, z are cylindrical coordinates, and $J_m(x)$ is a Bessel function. Then Eq. (5.2) becomes

$$\frac{1}{r'}\frac{d}{dr'}\left(r'\frac{dJ_m}{dr'}\right)(\cos m\varphi) f(z) e^{-i\omega\tau} - \left(\frac{m^2}{r'^2} f(z) - f''(z) - \frac{\omega^2}{u^2(z)} f(z)\right) \times J_m(Ar')(\cos m\varphi) e^{-i\omega\tau} = 0 . \tag{E2}$$

From the equation satisfied by the Bessel functions $J_m(x)$,

$$\frac{1}{A^2 r'}\frac{\partial}{\partial r'}\left(r'\frac{\partial J_m(Ar')}{\partial r'}\right) + \left(1 - \frac{m^2}{A^2 r'^2}\right) J_m(Ar') = 0 , \tag{E3}$$

we have

$$f'' + [\omega^2/u^2(z) - A^2]\, f = 0 . \tag{E4}$$

The boundary condition (5.3) implies

$$\frac{dJ_m(Ar')}{dr'}=0, \quad r'=a' \tag{E5}$$

$$f'(z)=0, \quad z=z_1, \quad 1+z_1 . \tag{E6}$$

The first equation yields

$$A_{mn}a'=\pi\alpha_{mn}, \tag{E7}$$

with[37]

$$\alpha_{00}=0, \quad \alpha_{10}=0.5861, \quad \alpha_{20}=0.9722, \quad \alpha_{01}=1.2197, \quad \alpha_{11}=1.6970, \quad \alpha_{02}=2.2331, \text{ etc.} \tag{E8}$$

We are left with the equation in z

$$f''+[\omega^2/u^2(z)-A_{mn}^2]f=0, \quad f'(z)=0, \quad z=z_1, \quad z=1+z_1, \tag{E9}$$

whose eigenvalue ω is the desired angular frequency. For a uniform velocity $u(z)=u_0$, we have

$$f=\cos B_p(z-z_1), \quad B_p=\pi p , \tag{E10}$$

$$\omega_{pmn}^2/u_0^2=A_{mn}^2+B_p^2=(\pi\alpha_{mn}/a')^2+(\pi p)^2 \tag{E11}$$

in dimensionless units. If a' is expressed in dimensional units we have

$$\omega_{pmn}^2/u_0^2=(\pi\alpha_{mn}/a')^2+(\pi p/h)^2 . \tag{E12}$$

The modes of the uniform system are classified by the three "quantum numbers" p, m, n, discussed in Sec. V.

For the nonuniform system we *define* the "average velocity" $\tilde{u}$ in terms of the eigenfrequency $\tilde{\omega}$, by Eq. (5.4) of the text, which is analogous to Eq. (E12). In order to find the eigenfrequency $\tilde{\omega}_{pmn}$ for a given mode, we have solved Eq. (E9) numerically for given values of t and $\tilde{\Delta}$, i.e., given $u(z)$. The method we used, which was devised by Wasserstrom,[38] introduces an auxiliary variable x, such that

$$u(z, x)=u_0(z)+\varphi(x)[u(z)-u_0(z)], \tag{E13}$$

where $\varphi(x)$ is a smooth function varying between 0 and 1 when x goes between 0 and 1. For $u_0(z)$ we choose the (constant) value of u in the absence of gravity (or its average value in the two-phase region). The differential equation (E9) for f is solved for successive values of x, starting from the known solution for $x=0$. In addition there is an auxiliary equation for the eigenvalue $\tilde{\omega}(x)$, whose value at $x=1$ is the desired solution. This method turns out to be quite convenient in practice, and permits us to find each mode of the resonator separately.

Special Case: Weak Gravity Effect

In the absence of gravity, the sound velocity u_0 is calculated from Eq. (5.1) expressed in terms of r and θ, and using the value of θ_0 derived from Eq. (C20). In the two-phase region we have $u_G=u_0(\theta=-1)$ and $u_L=u_0(\theta=+1)$. When the effect of gravity is weak, i.e., when $u(z)$ does not vary substantially between the bottom and top of the vessel, we may solve Eq. (E9) by perturbation theory in the small deviation

$$\eta(z)=1-u^2(z)/(u^2)_{\text{av}} , \tag{E14}$$

$$(u^2)_{\text{av}}=\int_{z_1}^{1+z_1}u^2(z)\,dz . \tag{E15}$$

It follows from lowest-order perturbation theory that for any mode $\{pmn\}$ we have

$$\tilde{u}_{pmn}^2=(u^2)_{\text{av}}\left(1-\int_{z_1}^{1+z_1}\eta(z)(\cos^2\pi pz)\,dz\right) . \tag{E16}$$

Thus, even in the limit of small gravity effect, the average velocity measured in the two-phase region will not necessarily be the simple average of u_G and u_L. Equation (E16) applied to the situation of constant values for u_G and u_L, i.e., to the two-phase region in the absence of gravity, yields

$$\tilde{u}_{pmn}=(1+z_1)u_G-z_1u_L , \quad p=0$$
$$\tilde{u}_{pmn}=(1+z_1)u_G-z_1u_L+(u_L-u_G)\frac{\sin 2\pi pz_1}{4\pi p} , \quad p\neq 0 \tag{E17}$$

to leading order in $(u_G-u_L)/\frac{1}{2}(u_G+u_L)\ll 1$.

---

*Present address (until March 1972): Theoretische Physik, Technische Universitaet München, 8046 Garching Bei München, Germany.

[1]A. Gouy, Compt. Rend. 115, 720 (1892).
[2]M. A. Weinberger and W. G. Schneider, Can. J. Chem. 30, 422 (1952); 30, 847 (1952).
[3]H. D. Baehr, Z. Elektrochem. 58, 416 (1954).
[4]M. Sh. Giterman and S. P. Malyshenko, Zh. Eksperim. i Teor. Fiz. 53, 2079 (1967) [Sov. Phys. JETP 26, 1176 (1968)].
[5]A. T. Berestov, M. S. Giterman, and S. P. Malyshenko, Zh. Eksperim. i Teor. Fiz. 56, 642 (1969) [Sov. Phys. JETP 29, 351 (1969)].
[6]A. T. Berestov and S. P. Malyshenko, Zh. Eksperim. i Teor. Fiz. 58, 2090 (1970) [Sov. Phys. JETP 31, 1127 (1970)].
[7]L. M. Artyukhovskaya, E. T. Shimanskaya, and Yu. I. Shimanskii, Zh. Eksperim. i Teor. Fiz. 59, 688 (1970) [Sov. Phys. JETP 32, 375 (1971)].
[8]A. V. Chalyi and A. D. Alekhin, Zh. Eksperim. i Teor. Fiz. 59, 337 (1970) [Sov. Phys. JETP 32, 181 (1971)]; B. Ya. Sukharevskii, A. V. Alapina, Yu. A. Dushechkin, T. N. Kharchenko, and I. S. Schetkin, *ibid.* 58, 1532 (1970) [*ibid.* 31, 820 (1970)].
[9]H. H. Schmidt, J. Chem. Phys. 54, 3610 (1971).
[10]R. B. Griffiths, Phys. Rev. 158, 176 (1967).
[11]M. Vicentini-Missoni, J. M. H. Levelt Sengers, and M. S. Green, J. Res. Natl. Bur. Std. (U.S.) 73A, 563

(1969).

[12]P. Schofield, J. D. Litster, and J. T. Ho, Phys. Rev. Letters 23, 1098 (1969).

[12a]For a general discussion of parametric equations of state see M. E. Fisher, *Proceedings of the* 1970 *Enrico Fermi Summer School on "Critical Phenomena"*, Varenna sul Lago di Como, Italy (Academic, New York, to be published).

[13]B. D. Josephson, J. Phys. C 2, 1113 (1969).

[14]P. Schofield, Phys. Rev. Letters 22, 606 (1969).

[15]A preliminary report was presented earlier: M. Barmatz and P. C. Hohenberg, Phys. Rev. Letters 24, 1225 (1970).

[16]A. V. Voronel', S. R. Garber, and L. D. Peretsman, Zh. Eksperim. i Teor. Fiz. 57, 92 (1969) [Sov. Phys. JETP 30, 54 (1970)], and references therein; A. V. Voronel', S. R. Garber, and U. M. Mamnitskii, *ibid.* 55, 2017 (1968) [*ibid.* 28, 1065 (1969)].

[17]The definitions presented here are only valid if the equation of state possesses the "lattice-gas" symmetry about $\rho = \rho_c$. For purposes of calculating the gravity effect this approximation is certainly sufficient. This matter is discussed briefly below. Note also that the normalization used for μ in Eq. (2.1) is different from the one employed in Ref. 15.

[18]D. S. Gaunt and C. Domb, J. Phys. C 3, 1442 (1970).

[19]M. S. Green, M. J. Cooper, and J. M. H. Levelt Sengers, Phys. Rev. Letters 26, 492 (1971).

[20]B. Widom and J. S. Rowlinson, J. Chem. Phys. 52, 1670 (1970); and private communication.

[21]N. D. Mermim and J. J. Rehr, Phys. Rev. Letters 26, 1155 (1971).

[22]J. A. Lipa, C. Edwards, and M. J. Buckingham, Phys. Rev. Letters 25, 1086 (1970).

[23]It is interesting to note that even the recent "best-fit" values of A, A', B_0, B_0' for the three-dimensional Ising model, presented by D. S. Gaunt and C. Domb [J. Phys. C 1, 1038 (1968)] have $B_0 \neq B_0'$. The ensuing singular term in C_v [Eq. (2.6c)] must be reconciled with correction terms obtained from analyzing other thermodynamic functions [cf. C. Domb in Ref. 12(a)].

[24]C. Edwards, J. A. Lipa, and M. J. Buckingham, Phys. Rev. Letters 20, 496 (1968).

[25]The definitions of t_0 employed in Refs. 24 and 15 differ slightly from Eq. (2.10), but they yield numbers of the same order of magnitude.

[26]A. M. Bykov, A. V. Voronel', V. A. Sonirov, and V. V. Shchekochikhina, Zh. Eksperim. i Teor. Fiz. Pis'ma v Redaktsiya 13, 33 (1971) [Sov. Phys. JETP Letters 13, 21 (1971)].

[27]S. G. Whiteway and S. G. Mason, Can. J. Chem. 31, 569 (1953).

[28]M. E. Fisher, J. Math. Phys. 5, 944 (1964), especially p. 950.

[29]H. W. Habgood and W. G. Schneider, Can. J. Chem. 32, 164 (1954).

[30]M. Barmatz, Phys. Rev. Letters 24, 651 (1970).

[31]M. Barmatz, *Critical Phenomena in Alloys, Magnets, and Superconductors*, edited by R. E. Mills, E. Ascher, and R. I. Jaffee (McGraw-Hill, New York, 1971), p. 541.

[32]See, for instance, T. Yamamoto, O. Tanimoto, Y. Yasuka, and K. Okada, in *Critical Phenomena, Proceedings of a Conference*, Natl. Bur. Std. Misc. Publ. No. 273, edited by M. S. Green and J. V. Sengers (U.S. GPO, Washington, D.C., 1966), p. 86; D. Teany, V. L. Moruzzi, and B. E. Argyle, J. Appl. Phys. 37, 1122 (1967); B. Golding, *ibid.* 42, 1381 (1971); and Phys. Rev. Letters 27, 1142 (1971); D. L. Connelly, J. S. Loomis, and D. E. Mapother, Phys. Rev. B 3, 924 (1971).

[33]J. M. H. Levelt Sengers, J. Straub, and M. Vicentini-Missoni, J. Chem. Phys. 54, 5034 (1971).

[34]E. H. W. Schmidt, in Ref. 32, p. 13; J. Straub, Ph.D. thesis (München, 1965) (unpublished).

[34a]We are indebted to Dr. H. Kierstead for pointing out this simplification, valid for arbitrary values of b^2. Use of Eq. (A7b) in Eqs. (D5), (D6), and (D19)–(D28) would simplify the algebra. However, since our numerical calculations were performed before we were aware of Eq. (A7b), we have kept the more complicated equations in the text.

[35]E. Isaacson and H. B. Keller, *Analysis of Numerical Methods* (Wiley, New York, 1966), p. 97.

[36]We are using the same notation for the function S_s in terms of the variables t and z, and the variables r and θ. No confusion should arise since we indicate the arguments explicitly.

[37]See, for instance P. M. Morse, *Vibration and Sound* (McGraw-Hill, New York, 1948), p. 399.

[38]E. Wasserstrom, J. Computational Phys. 9, 53 (1972).